

---

# Noise to the Rescue: Escaping Local Minima in Neurosymbolic Local Search

---

Alessandro Daniele<sup>1</sup> Emile van Krieken<sup>2</sup>

## Abstract

Deep learning has achieved remarkable success across various domains, largely thanks to the efficiency of backpropagation (BP). However, BP’s reliance on differentiability poses challenges in neurosymbolic learning, where discrete computation is combined with neural models. We show that applying BP to Gödel logic, which represents conjunction and disjunction as min and max, is equivalent to a local search algorithm for SAT solving, enabling the optimisation of discrete Boolean formulas without sacrificing differentiability. However, deterministic local search algorithms get stuck in local optima. Therefore, we propose the *Gödel Trick*, which adds noise to the model’s logits to escape local optima. We evaluate the Gödel Trick on SATLIB, and demonstrate its ability to solve a broad range of SAT problems. Additionally, we apply it to neurosymbolic models and achieve state-of-the-art performance on Visual Sudoku, all while avoiding expensive probabilistic reasoning. These results highlight the Gödel Trick’s potential as a robust, scalable approach for integrating symbolic reasoning with neural architectures.

## 1. Introduction

Deep learning has revolutionised artificial intelligence, producing state-of-the-art results in a wide range of tasks. A key factor behind this success is the efficiency of backpropagation (BP) (Rumelhart et al., 1986), which enables end-to-end optimisation of neural models. However, BP fundamentally relies on differentiability, restricting its applicability to continuous functions.

This issue is especially critical in *neurosymbolic integration* (NeSy), where the inherently discrete nature of symbolic reasoning needs to be effectively integrated with neural

networks (Feldstein et al., 2024; Marra et al., 2024). A promising approach within the NeSy field uses fuzzy logic to bridge the gap between continuous and discrete representations (van Krieken et al., 2022; Badreddine et al., 2022; Daniele and Serafini, 2019).

Fuzzy logic generalizes classical logic by allowing continuous truth values, enabling differentiable reasoning. However, this approach leads to an approximation of discrete logical reasoning, as no fuzzy logic fully satisfies all properties of classical logic (Gupta and Qi, 1991). This issue has limited the applicability of fuzzy logic in NeSy, as the approximations may not always align well with the intended logical behaviour (van Krieken et al., 2022).

In our work, we show that Gödel logic, a specific fuzzy semantics that simply uses the minimum and maximum, is a notable exception. Gödel logic retains most desirable properties of classical logic while being differentiable, making it a compelling candidate for NeSy. Specifically, we demonstrate that there is a consistent mapping from fuzzy truth values to Boolean ones that provides a bridge between the continuous and discrete worlds.

Furthermore, we prove that BP applied to Gödel logic behaves like a purely discrete search method. Specifically, we draw parallels between the gradient-based updates in Gödel logic and variable flips applied by *local search algorithms* (LSAs), a well-known family of meta-heuristics for SAT solving (Hoos and Stützle, 2000a). This allows us to interpret the training process as discrete search.

Analysing Gödel logic from this perspective reveals its main limitation: like some LSAs (e.g., GSAT (Hoos and Stützle, 2000a)), it converges to local minima, after which it stops making progress. To escape these local minima, we propose the *Gödel Trick*, a reparameterisation trick (Mohamed et al., 2020; Kingma and Welling, 2014) that defines a continuous probability distribution over fuzzy truth values to introduce exploration.

We evaluate Gödel Trick on many SAT solving benchmarks (Hoos and Stützle, 2000b). Moreover, we show that Gödel Trick can be used to incorporate prior symbolic knowledge in neural networks through the Visual Sudoku task (Augustine et al., 2022), a challenging NeSy task. In both settings, our approach demonstrates robust performance and scala-

<sup>1</sup>Fondazione Bruno Kessler, Trento, Italy <sup>2</sup>University of Edinburgh, Edinburgh, United Kingdom. Correspondence to: Alessandro Daniele <daniele@fbk.eu>.

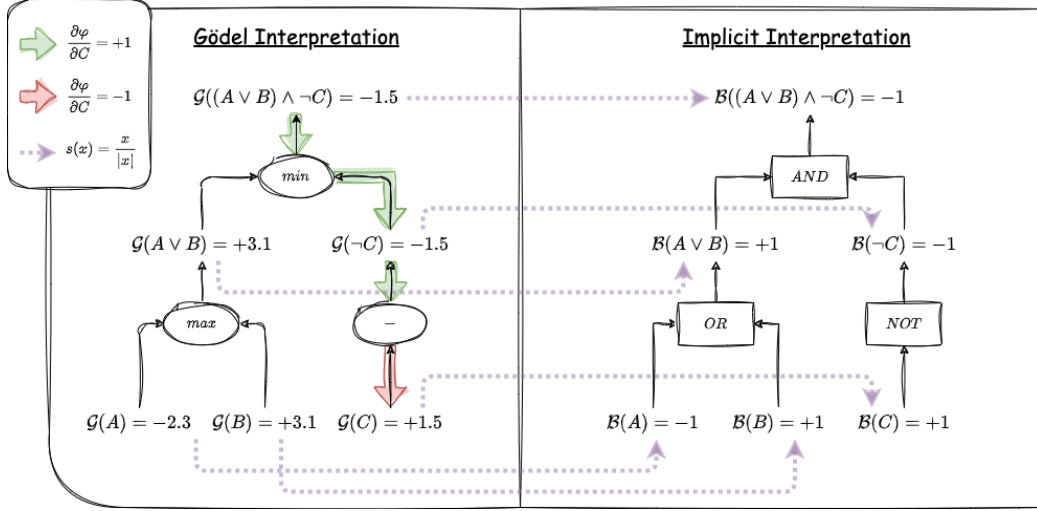


Figure 1. Example of Gödel interpretation (left) and corresponding implicit interpretation (right) for the formula  $\varphi = (A \vee B) \wedge \neg C$ . Each truth value in the implicit interpretation is either a  $-1$  (false) or a  $+1$  (true), and it can be computed via the sign function applied on the corresponding continue value in the Gödel interpretation.

bility, suggesting that the Gödel Trick, and potentially other variants of Gödel logic, offer a promising avenue for integrating symbolic reasoning into neural architectures.

In Section 2 we introduce the background; in Section 3 the related work; Section 4 the relation between Gödel and Boolean logic; Section 5 Gödel Logic in comparison with LSAs; Section 6 the Gödel Trick; Sections 7-8 the experimental analysis; finally Section 9 the conclusions.

## 2. Background

### 2.1. Propositional logic

We define the syntax of a logic formula  $\varphi$  recursively as follows:  $\varphi ::= p \mid \neg\psi \mid (\psi_1 \wedge \psi_2) \mid (\psi_1 \vee \psi_2)$ , where  $p \in P$  is an atomic proposition,  $\neg$  is negation,  $\wedge$  is conjunction (AND), and  $\vee$  is disjunction (OR), and  $\psi_i$  are subformulas.

In classical logic, an interpretation  $\mathcal{B}(p) \in \{-1, +1\}$  assigns a truth value to each propositional variable  $p \in P$ , where  $-1$  and  $+1$  represent false and true, respectively. The truth value of a formula is found by:

$$\begin{aligned} \mathcal{B}(p) &\in \{-1, +1\} \\ \mathcal{B}(\neg\varphi) &= \text{NOT}(\mathcal{B}(\varphi)) \\ \mathcal{B}(\varphi \wedge \psi) &= \text{AND}(\mathcal{B}(\varphi), \mathcal{B}(\psi)) \\ \mathcal{B}(\varphi \vee \psi) &= \text{OR}(\mathcal{B}(\varphi), \mathcal{B}(\psi)) \end{aligned}$$

### 2.2. Gödel logic semantics

Gödel logic generalises classical logic by allowing truth values to be real numbers in  $[0, 1]$ , where 0 represents false, 1 represents true, and intermediate values are par-

tially true. It is a fuzzy logic based on  $t$ -norms and  $t$ -conorms, which are associative and commutative operations that generalise conjunction and disjunction to continuous values (Klement et al., 2013). Specifically, the Gödel logic interprets conjunction, disjunction and negation as  $\min$ ,  $\max$  and  $1 - x$  respectively. The  $\min$  and  $\max$  are the only *idempotent* fuzzy operators: they satisfy  $\min(x, x) = x$  and  $\max(x, x) = x$  for all  $x \in [0, 1]$ . Furthermore, the minimum and maximum is the only pair of fuzzy operators that is *distributive*:  $\min(x, \max(y, z)) = \max(\min(x, y), \min(x, z))$  (Klement et al., 2013).

In the remainder, we adopt truth values of formulas over the real number space  $\mathbb{R}$  instead of the interval  $[0, 1]$ . Specifically, we consider logits in  $\mathbb{R}$ , that is, the outputs of a neural network before applying the sigmoid function (see Appendix A.1 for more details).

Formally, an interpretation  $\mathcal{G}$  in Gödel logic defines a truth value in  $\mathbb{R}$  for each propositional variable  $p \in P$  and computes the truth value of each formula  $\varphi$  recursively as:

$$\begin{aligned} \mathcal{G}(p) &\in \mathbb{R}, \\ \mathcal{G}(\neg\varphi) &= -\mathcal{G}(\varphi), \\ \mathcal{G}(\varphi \wedge \psi) &= \min(\mathcal{G}(\varphi), \mathcal{G}(\psi)), \\ \mathcal{G}(\varphi \vee \psi) &= \max(\mathcal{G}(\varphi), \mathcal{G}(\psi)). \end{aligned}$$

## 3. Related work

Neurosymbolic integration (NeSy) studies how to integrate neural networks with symbolic reasoning (Marra et al., 2024; Feldstein et al., 2024). To this end, it is common to use differentiable logics (Slusarz et al., 2023), which can roughly be divided into fuzzy and probabilistic logics.

**Differentiable fuzzy logics** like LTN and SBR permit a large choice of fuzzy logics, including Gödel and variants of the product logic (Badreddine et al., 2022; Diligenti et al., 2017). These create differentiable loss functions to train neural networks. The choice of fuzzy logic operator has been studied theoretically and empirically (van Krieken et al., 2022; Grespan et al., 2021; Flinkow et al., 2024; Slusarz et al., 2023). Furthermore, fuzzy logic operators can be used as part of the neural network architecture itself to incorporate background knowledge (Giunchiglia et al., 2024; Daniele and Serafini, 2019; Daniele et al., 2023b). None of the aforementioned methods add noise to the fuzzy logic operators.

Many other methods use **probabilistic logics**, such as Semantic Loss (Xu et al., 2018), DeepProbLog (Manhaeve et al., 2018) and Semantic Probabilistic Layers (Ahmed et al., 2022). These methods require computing the weighted model counting (Chavira and Darwiche, 2008), a #P-hard problem (Valiant, 1979), at each iteration. To overcome this, methods either use compiled probabilistic circuits (Choi et al., 2020; Kisa et al., 2014) or use approximations, for example via neural networks (van Krieken et al., 2023) or by sampling (De Smet et al., 2023). Maene et al. (2024) compared various approximations, including fuzzy logics and the Gumbel-Softmax, a reparameterisation-based method similar to the Gödel trick.

## 4. Relation between Gödel and Boolean Logics

In this section, we demonstrate that the sign function creates a way of interpreting Gödel logic in terms of classical logic. Because of this relation, we can map the continuous interpretations of Gödel logic to discrete boolean interpretations of classical logic. In the case of the Gödel logic, we consider  $\mathbb{R} \setminus \{0\}$ , since this relation can only be proved when we exclude zero. In practice, this is not an issue since we introduce noise during training, making the probability of  $\mathcal{G}(\varphi) = 0$  negligible (see Section 6).

The sign function  $s : \mathbb{R} \setminus \{0\} \rightarrow \{-1, 1\}$  is defined as:

$$s(x) = \frac{x}{|x|} = \begin{cases} -1, & \text{if } x < 0, \\ 1, & \text{if } x > 0. \end{cases}$$

**Theorem 4.1.** *Consider a Gödel interpretation  $\mathcal{G}$ . Define the Boolean interpretation  $\mathcal{B}$  obtained by setting  $\mathcal{B}(p) = s(\mathcal{G}(p))$  for all propositional variables  $p \in P$ . Then for all formulas  $\varphi$ , we have  $s(\mathcal{G}(\varphi)) = \mathcal{B}(\varphi)$ .*

For proof, see Appendix A.2.

### 4.1. Implicit interpretation

The relation defined in the previous section plays a crucial role in enabling backpropagation (BP) to optimise logical

formulas in a differentiable setting. At each step of the BP algorithm, the current Gödel interpretation  $\mathcal{G}(\varphi)$  can be mapped to a corresponding discrete interpretation via the sign function. We call this discrete interpretation the *implicit interpretation*, defined as  $\mathcal{B}(\varphi) = s(\mathcal{G}(\varphi))$ .

*Example 1.* Let  $\varphi$  be the formula  $\varphi = (A \vee B) \wedge \neg C$ . Let the Gödel interpretation for the propositions be:

$$\mathcal{G}(A) = -2.3 \quad \mathcal{G}(B) = 3.1 \quad \mathcal{G}(C) = 1.5$$

The discrete interpretation is obtained by applying the sign function  $s$ :

$$\mathcal{B}(A) = -1 \quad \mathcal{B}(B) = +1 \quad \mathcal{B}(C) = +1$$

We show in Figure 1 that each node of the computational graph of the Gödel interpretation is connected by a violet arrow (representing  $s$ ) to a corresponding node in the implicit interpretation. Note that, for all the formulas in the implicit interpretation, the truth value is consistent with classical logic operators’ semantics.

The existence of the implicit interpretation has profound implications for the way we understand BP applied on Gödel logic interpretations. At each step of the optimisation process, a discrete interpretation can be derived, meaning that BP on Gödel logic is symbolically grounded.

## 5. Backpropagation on Gödel Logic

In this section, we analyse the behaviour of backpropagation (BP) applied to Gödel logic. We first show that the gradients are sparse, affecting only one propositional variable at each optimisation step. Then, we analyse the direction of the gradients and draw a parallel with local search algorithms for SAT, showing a consistent behaviour between BP on Gödel logic and purely discrete search.

With abuse of notation, we will refer to the interpretation of a formula by ignoring the function  $\mathcal{G}$  when computing the partial derivatives, e.g.,  $\frac{\partial \mathcal{G}(\varphi)}{\partial \mathcal{G}(\psi)}$  is reported as  $\frac{\partial \varphi}{\partial \psi}$ .

### 5.1. Sparse gradients

Given a formula  $\varphi$ , the computation graph of its Gödel interpretation contains a set of paths that connect it to the atomic propositions on which it depends. In this subsection, we show that during training, only one such path is *active*; i.e., it has a gradient different than zero. First, we define the concept of *path*.

**Definition 5.1 (Path).** A *path*  $\mathcal{P}$  from a formula  $\varphi$  to an atomic proposition  $p$  is a sequence of formulas:

$$\mathcal{P} = (\varphi, \psi_1, \psi_2, \dots, p),$$

where each  $\psi_i$  is a direct subformula of  $\psi_{i-1}$ , and  $p$  is an atomic proposition.

Given a path  $\mathcal{P} = (\varphi, \psi_1, \psi_2, \dots, p)$ , the partial derivative of  $\varphi$  with respect to  $p$  along the path is given by

$$\frac{\partial \varphi}{\partial p} = \frac{\partial \varphi}{\partial \psi_1} \cdot \frac{\partial \psi_1}{\partial \psi_2} \cdot \dots \cdot \frac{\partial \psi_{n-1}}{\partial p},$$

obtained by applying the chain rule.

Each partial derivative  $\frac{\partial \psi_i}{\partial \psi_{i+1}}$  corresponds to either a min, max, or negation operation. The negation will have a derivative of  $-1$ , while the subformulas of the min and max will have a derivative of 1 or 0 depending on which subformula is selected as the minimum or maximum.

Consistent with PyTorch, we resolve the case where  $\mathcal{G}(\psi_1) = \mathcal{G}(\psi_2)$  by randomly selecting which partial derivative is zero and one. This can happen when  $\psi_1$  and  $\psi_2$  depend on a common subformula<sup>1</sup>, like  $\varphi = \psi_1 \wedge \psi_2$ , with  $\psi_1 = A \vee B$  and  $\psi_2 = B \vee C$ . If  $\mathcal{G}(B)$  is larger than both  $\mathcal{G}(A)$  and  $\mathcal{G}(C)$ , then the truth values of  $\psi_1$  and  $\psi_2$  are both equal to  $\mathcal{G}(B)$ . This choice makes no difference for the final gradient, since both paths end in  $\mathcal{G}(B)$ , as the following theorem shows (proof in Appendix A.3).

**Theorem 5.2.** *The partial derivative  $\frac{\partial \varphi}{\partial \psi_i}$ , as calculated along a path  $\mathcal{P} = (\varphi, \psi_1, \dots, p)$ , takes values in  $\{-1, 0, 1\}$ . If different from zero, then the sign of the gradient is positive iff the number of the negations in the path is even:*

$$\frac{\partial \varphi}{\partial \psi_i} = (-1)^n$$

with  $n$  the number of negations in the subpath from  $\varphi$  to  $\psi_i$ .

**Definition 5.3** (Active path). A path  $\mathcal{P} = (\varphi, \psi_1, \psi_2, \dots, p)$  is *active* if the partial derivative  $\frac{\partial \varphi}{\partial p}$  is different from zero. Conversely, a path with derivative zero is called *inactive*.

**Theorem 5.4.** *Given a formula  $\varphi$ , there is a unique active path  $\mathcal{P} = (\varphi, \psi_1, \dots, p)$  in the computational graph of  $\varphi$ .*

For a full proof, see Appendix A.4. This result previously appeared in a different form (van Krieken et al., 2022).

*Example 2.* Consider the formula and interpretation of Example 1. The interpretation for the formula  $\varphi = (A \vee B) \wedge \neg C$  is  $-1.5$ , obtained as the minimum between  $\mathcal{G}(A \vee B) = 3.1$  and  $\mathcal{G}(\neg C) = -1.5$ . Since  $A \vee B$  does not correspond to the minimal value, the partial derivative with respect to node  $A \vee B$  is zero, and none of the paths passing through it is active. The unique active path reaches  $\mathcal{G}(C)$ , denoted by green and red arrows in Figure 1. Note that the partial derivatives are positive (green) before reaching the negation, and negative (red) after as predicted by Theorem 5.2.

<sup>1</sup>Note that, the probability of two atomic formulas having equal value is neglectable. Moreover, in such a case, the problem would arise at a single training step, having little to no influence on the training process.

Theorem 5.4 tells us there is a unique path active at each step of BP. However, it does not tell us whether the applied change is positive or negative. While Theorem 5.2 partially answer the question, we can show that the partial derivative of a formula  $\varphi$  w.r.t. another formula  $\pi$  can be computed directly from the implicit interpretations of the two formulas.

**Theorem 5.5.** *Let  $\varphi$  be a formula, and let  $\pi$  be a subformula in the active path of  $\varphi$ . The partial derivative  $\frac{\partial \varphi}{\partial \pi}$  is equal to the product of the implicit interpretation of the two formulas:*

$$\frac{\partial \varphi}{\partial \pi} = \mathcal{B}(\varphi) \cdot \mathcal{B}(\pi)$$

Theorem 5.5 (proof: Appendix A.5) shows that the direction of the gradient on a specific formula depends exclusively on the implicit interpretation. More precisely, assuming  $\pi$  is in an active path, if the formula is satisfied ( $\mathcal{B}(\varphi) = 1$ ), the derivative will be positive if  $\pi$  is positive and negative otherwise. BP will only modify the truth values by increasing their magnitude, but will not change their sign. In contrast, if the formula is not satisfied ( $\mathcal{B}(\varphi) = -1$ ), the direction of the gradient is the negation of the boolean interpretation; i.e.,  $\frac{\partial \varphi}{\partial \pi} = -\mathcal{B}(\pi)$ . Hence, it moves the current truth value of  $\pi$  in the direction of the threshold, potentially flipping the corresponding boolean truth value.

Theorem 5.5 provides one method for computing the direction of the partial derivatives along an active path  $\mathcal{P}$ . Theorem 5.2 proposes an alternative method:  $\frac{\partial \varphi}{\partial \pi} = (-1)^n$ , where  $n$  is the number of negations in the subpath from  $\varphi$  to  $\pi$ . What if these two methods do not agree? Then  $\mathcal{P}$  can not be an active path. To show this, we first define the concepts of *representation* of a discrete interpretation and of *candidate path*.

**Definition 5.6** (Representation of a discrete interpretation). Let  $\mathcal{B}$  be a boolean interpretation and  $\mathcal{G}$  a Gödel interpretation. If, for every formula  $\varphi$ ,  $\mathcal{B}(\varphi) = s(\mathcal{G}(\varphi))$ , then  $\mathcal{G}$  is called a *representation* of  $\mathcal{B}$ .

**Definition 5.7** (Candidate Path). A path  $\mathcal{P} = (\varphi, \psi_1, \dots, p)$  is a *candidate path* for formula  $\varphi$  with boolean interpretation  $\mathcal{B}$  if there exists a representation  $\mathcal{G}$  of  $\mathcal{B}$  such that  $\mathcal{P}$  is the active path of  $\mathcal{G}$ .

**Theorem 5.8.** *Let  $\varphi$  be a formula and  $\psi_m$  a subformula of  $\varphi$ . Let  $\mathcal{P} = (\varphi, \psi_1, \psi_2, \dots, \psi_m)$  be the path from  $\varphi$  to  $\psi_m$  and  $n_i$  be the number of negations in the subpath  $(\varphi, \psi_1, \psi_2, \dots, \psi_i)$ . If there is an  $i \in \{1, \dots, m\}$  such that*

$$\mathcal{B}(\varphi) \cdot \mathcal{B}(\psi_i) \neq (-1)^{n_i}$$

*then  $\mathcal{P}$  is not a candidate path for  $\mathcal{B}$ .*

*Proof.* Assume otherwise, that  $\mathcal{P}$  is the active path of some representation  $\mathcal{G}$  of  $\mathcal{B}$ . Then for each subformula  $\psi_i$  in the

path, by Theorem 5.5 (LHS) and Theorem 5.2 (RHS) we have that

$$\mathcal{B}(\varphi) \cdot \mathcal{B}(\psi_i) = \frac{\partial \varphi}{\partial \psi_i} = (-1)^{n_i}.$$

But this contradicts the assumption, and therefore  $\mathcal{P}$  is not a candidate path.  $\square$

For an example, see Appendix B (Example 4).

## 5.2. BP on CNFs formulas

Although BP on Gödel logic can be applied to any rule, it is especially worth analysing its behaviour in the context of CNF formulas.

**Corollary 5.9.** *Let  $\varphi$  be a formula expressed in CNF*

$$\varphi = \bigwedge_{i=1, \dots, m} c_i$$

where  $c_i$  represent the  $i^{\text{th}}$  clause, and  $\mathcal{B}$  a boolean interpretation. If  $\varphi$  is not satisfied ( $\mathcal{B}(\varphi) = -1$ ), the active path passes through an unsatisfied clause.

*Proof.* For each clause  $c_i$ , the corresponding number  $n_i$  of negations in the subpath from  $\varphi$  to  $c_i$  is zero, and  $(-1)^{n_i} = 1$ . Hence, in order to be part of an active path,  $\mathcal{B}(c_i)$  must be negative (by applying Theorem 5.8).  $\square$

Note that the corollary just proposes a necessary condition for a path to be candidate. But is it also a sufficient condition? In other words, is there a candidate path for all literals of unsatisfied clauses? The answer to this question is negative. We show this with a counterexample (Example 5 in Appendix B): when a clause containing a variable is a logical consequence of other clauses, the value of that variable is always irrelevant for the interpretation of formula  $\varphi$ .

**Definition 5.10** (Relevant clause). A clause  $c$  is a logical consequence of another clause  $c'$  if all the literals of  $c'$  are also in  $c$ :  $l \in c' \rightarrow l \in c$ . A clause  $c$  is *relevant* in  $\varphi$  if it is not a logical consequence of another clause  $c'$  in  $\varphi$ .

We can now update the previous question: is there a candidate path for all the literals of unsatisfied relevant clauses? This time, the answer is affirmative (proof in Appendix A.6).

**Theorem 5.11.** *Let  $\varphi$  be a formula expressed in CNF and  $\mathcal{B}$  a boolean interpretation. Let  $\mathcal{P} = (\varphi, c, l)$  be a path from  $\varphi$  to a literal  $l$ . If clause  $c$  is relevant and it is not satisfied in  $\mathcal{B}$  ( $\mathcal{B}(c) = -1$ ), then  $\mathcal{P}$  is a candidate path for  $\varphi$  and  $\mathcal{B}$ .*

## 5.3. Comparison with common LSAs

### Algorithm 1 Local Search for SAT

---

```

1: Input: formula in CNF  $\varphi$ , maximum iterations  $max\_iter$ 
   Output: Satisfying interpretation or failure
2: Randomly initialise interpretation  $\mathcal{B}$ 
3: for  $i = 1$  to  $max\_iter$  do
4:   Evaluate interpretation  $\mathcal{B}$  on  $\varphi$ 
5:   if  $\varphi$  is satisfied by  $\mathcal{B}$  then
6:     return  $\mathcal{B}$ 
7:   else
8:     Select proposition  $p$  from an unsatisfied clause
9:     Update  $\mathcal{B}$  by flipping the truth value of  $p$ 
10: return failure
    
```

---

In the previous section, we saw that BP applied on Gödel interpretations mimics the behaviour of local search algorithms for SAT, thanks to the sparsity of the gradients of Gödel logic. When applied to a CNF, both approaches iteratively select an unsatisfied clause and flip the truth value of one of its propositions. What is different is the selection heuristic: instead of relying on, for instance, the count of satisfied clauses, BP chooses the variable based on continuous truth values given by the Gödel interpretation. One consequence of this difference is that BP does not require a specific normal form like CNF to optimise logical formulas. This is particularly advantageous, as converting arbitrary formulas to CNF can lead to an exponential increase in the number of clauses (Biere et al., 2009).

However, the real advantage of optimising Gödel logic with BP lies in the option of seamlessly integrating combinatorial optimisation within neural network frameworks, since NNs are also optimised through BP. Indeed, unlike standard LSAs, which are purely symbolic methods, Gödel logic provides a differentiable framework where combinatorial optimisation emerges naturally by applying BP.

## 5.4. Local minima and cycles

Local search algorithms for SAT often converge to local minima. BP on Gödel logic faces a similar problem, but instead of being trapped in a single discrete solution, it often oscillates between two distinct interpretations. This behaviour arises due to the nature of the BP updates in Gödel logic, where certain variables are repeatedly adjusted in response to small variations in their truth values.

*Example 3.* Consider the formula:  $\varphi = (A \vee B) \wedge (\neg B \vee C)$ . If the initial truth values of  $A$  and  $C$  are very low, then  $B$  becomes the main variable affected by BP updates. Since must be true for the first conjunct and false for the second conjunct, the gradient updates will cause to constantly switch between  $-1$  and  $+1$ . This leads to an oscillatory behaviour instead of convergence to a stable solution.

## 6. The Gödel Trick

The **Gödel Trick** (GT) introduces a controlled perturbation to the Gödel interpretation of a proposition, enabling stochastic exploration of the solution space to escape local minima. Formally, we define the perturbed interpretation:

$$\begin{aligned}\mathcal{G}_\epsilon(p) &= \mathcal{G}(p) + \epsilon, \\ \mathcal{G}_\epsilon(\neg\varphi) &= -\mathcal{G}_\epsilon(\varphi), \\ \mathcal{G}_\epsilon(\varphi \wedge \psi) &= \min(\mathcal{G}_\epsilon(\varphi), \mathcal{G}_\epsilon(\psi)), \\ \mathcal{G}_\epsilon(\varphi \vee \psi) &= \max(\mathcal{G}_\epsilon(\varphi), \mathcal{G}_\epsilon(\psi)).\end{aligned}$$

where  $\epsilon$  is a noise term preventing cycles. The Gödel Trick is a reparametrisation trick (Kingma and Welling, 2014), where the expected value of the gradient of a formula  $\varphi$  corresponds to the gradient of the expected value of  $\varphi$ :  $\mathbb{E}_\epsilon [\nabla_{\mathcal{G}(p)} \mathcal{G}_\epsilon(\varphi)] = \nabla_{\mathcal{G}(p)} \mathbb{E}_\epsilon [\mathcal{G}_\epsilon(\varphi)]$ . This can be derived from standard results on pathwise gradient estimators (Mohamed et al., 2020).

### 6.1. Gödel Trick as approximate probabilistic inference

In Section 4, we proved that the sign function  $s$  allows the mapping of a Gödel interpretation to a discrete implicit one. Similarly, a continuous probability distribution over Gödel interpretation can be mapped to an *implicit* discrete distribution over Boolean interpretations:  $\mathcal{B}_\epsilon(\varphi) = s(\mathcal{G}_\epsilon(\varphi))$ .

For a proposition  $p$ , the probability  $P(\mathcal{B}_\epsilon(p))$  of  $p$  being true under the implicit distribution  $\mathcal{B}_\epsilon$  is:

$$\begin{aligned}P(\mathcal{B}_\epsilon(p)) &= P(\mathcal{G}_\epsilon(p) > 0) = P(\mathcal{G}(p) + \epsilon > 0) \quad (1) \\ &= 1 - F_\epsilon(-\mathcal{G}(p)) = \theta_\epsilon(\mathcal{G}(p)). \quad (2)\end{aligned}$$

where  $F_\epsilon$  is the cumulative distribution function (CDF) of  $\epsilon$ , and  $\theta_\epsilon(x) = 1 - F_\epsilon(-x)$  is the function that maps the unperturbed truth value  $\mathcal{G}(p)$  of a proposition  $p$ , to the probability of  $p$  being true according to  $\mathcal{B}_\epsilon$ .

We want now to establish a connection between the implicit distribution  $\mathcal{B}_\epsilon$  and probabilistic inference. First, we define the interpretation of a formula under probabilistic logic.

**Definition 6.1** (Probabilistic logic). Let  $\varphi$  be a formula defined over some propositions  $p_i$ . Let  $\pi_i$  be the probability associated with proposition  $p_i$ . Then, the probability associated to  $\varphi$  under probabilistic logic is defined as:

$$P(\varphi) = \sum_{\omega \in \{-1,1\}^n} H(\mathcal{B}(\varphi; \omega)) P(\omega) \quad (3)$$

$$P(\omega) = \prod_{i=1}^n \pi_i^{H(\omega_i)} (1 - \pi_i)^{1-H(\omega_i)} \quad (4)$$

where  $H$  is the Heaviside function that maps positive values to one, and negative values to zero:  $H(x) = \mathbf{1}(x > 0)$ ; and  $\mathcal{B}(\varphi; \omega)$  represents the classic interpretation of  $\varphi$ , as defined in Section 2.1, assuming  $\omega$  to be the vector containing the interpretations of propositions:  $\mathcal{B}(p_i) = \omega_i$ .

The connection between GT and probabilistic logic is given by the following theorem.

**Theorem 6.2.** Let  $\varphi$  be a formula defined over some propositions  $p_i$ . Let  $\varphi$  be interpreted under probabilistic logic, with  $\pi_i$  the probability associated with proposition  $p_i$ , and let  $\epsilon$  be a continuous distribution over the real numbers.

If we define the proposition’s truth values as  $\mathcal{G}(p_i) = \theta_\epsilon^{-1}(\pi_i)$ , then:

$$P(\mathcal{B}_\epsilon(\varphi)) = P(\varphi)$$

where  $P(\varphi)$  is the probability of  $\varphi$  being true under the probabilistic interpretation.

*Proof.* The proof is a direct consequence of Theorem 4.1, and it is formally derived in Appendix A.7.  $\square$

### 6.2. The choice of the noise distribution

The noise  $\epsilon$  plays a crucial role in the GT. In this work, we consider two options: logistic and uniform distributions.

#### 6.2.1. LOGISTIC DISTRIBUTION

For a standard logistic distribution, the corresponding CDF is the sigmoid function  $F_\epsilon(x) = \sigma(x) = \frac{1}{1+e^{-x}}$ , hence:

$$\theta_\epsilon(\mathcal{G}(p)) = 1 - F_\epsilon(-\mathcal{G}(p)) \quad (5)$$

$$= 1 - \sigma(-\mathcal{G}(p)) = \sigma(\mathcal{G}(p)) \quad (6)$$

Thus, in the logistic noise case,  $\mathcal{G}(p)$  can be interpreted as the logit of the probability of  $p$  being true, establishing a direct link between the GT and probabilistic inference. Moreover, since the logistic distribution can be expressed as the difference of two Gumbel distributions, one can establish a connection between the Gödel Trick and the Gumbel-Max Trick (Gumbel, 1954), a common reparametrisation method for estimating expected values in discrete settings. This connection is shown in Appendix D for the broader scenario introduced in Appendix C.

#### 6.2.2. UNIFORM DISTRIBUTION

The probability mass of the logistic distribution is concentrated close to the center, potentially reducing the exploration effect of the noise. Therefore, we also consider the uniform distribution, which is more spread out, potentially increasing the exploration of the solution space.

Note that the probabilistic interpretation of GT holds for distributions other than the logistic, as highlighted by Equation 2. However, we can no longer directly interpret  $\mathcal{G}(p)$  as the logits of  $P(p)$  as it induces a different discrete distribu-

tion. Specifically, if  $\epsilon \sim \mathcal{U}(a, b)$ :

$$\theta_\epsilon(x) = \begin{cases} 0 & \text{if } x < -b \\ \frac{x+b}{b-a} & \text{if } x \in [-b, -a] \\ 1 & \text{if } x > -a. \end{cases} \quad (7)$$

Given a probability  $\pi$  of a proposition  $p$ , the unperturbed truth value is  $\theta_\epsilon^{-1}(\pi) = \pi \cdot (b - a) - b$ .

## 7. Experiments on SAT

In this section, we evaluate the performance of the GT method on SAT problems. Specifically, we applied our approach to all satisfiable benchmarks available in the SATLIB library (Hoos and Stützle, 2000b). The choice of satisfiable instances is motivated by the fact that GT is an incomplete method for SAT. However, it is worth noting that most of the problems in SATLIB are satisfiable, as many SAT solvers themselves are incomplete.

### 7.1. Setup

SATLIB is a well-established repository containing various benchmark collections for the SAT problem. Each collection represents a distinct domain. For example, the UF family consists of randomly generated 3-SAT problems and includes 10 benchmarks of varying sizes. The Planning collection, on the other hand, comprises SAT-encoded planning problems. Each benchmark in SATLIB consists of multiple SAT problem instances.

We compare GT against three different fuzzy semantics: Product, Łukasiewicz, and Gödel logics. Additionally, for the GT, we experimented with both the Uniform and Logistic noise distributions.

### 7.2. Methodology

Initially, we conducted a grid search to optimise hyperparameters. This search was performed separately for each method on the simplest benchmark of the UF collection: `uf20-91`. We run all the SAT experiments on an NVIDIA RT2080Ti with 11GB of RAM.

Figure 2 shows the percentage of solved problems for each method as a function of the number of training epochs. The reported averages are computed over 100 samples (equivalent to 100 independent runs), each evaluated on the 1000 instances of SAT in `uf20-91`. Among the baselines, Product performs best, followed by Gödel, while Łukasiewicz fails to solve any instance. Notably, both GT variants significantly outperform all baselines, with GT-Uniform solving almost all instances. These results align with theoretical expectations: Gödel logic tends to converge quickly to sub-optimal solutions, whereas the noise introduced in GT-based models facilitates better exploration.

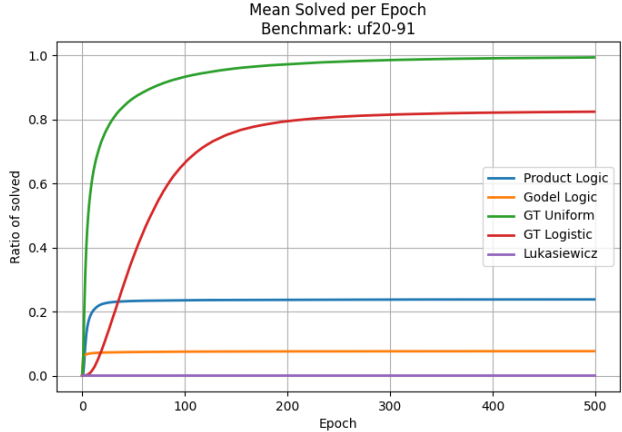


Figure 2. Ratio of solved problems on the `uf20-91` benchmark of SATLIB. Average of 100 runs over 50k epochs (granularity: 100 epochs).

We then applied all methods, excluding Łukasiewicz due to its complete failure, to the remaining SATLIB benchmarks. The results are summarized in Table 1. The table reports the average performance across benchmark collections and includes the top-performing GT variant and the best baseline, the Product logic, which fail on almost all benchmarks except for the simplest instances in the UF family.

Domain	Product Logic		GT Uniform	
	S(%)	B(%)	S(%)	B(%)
UF	2.9 ± 7.4	6.6 ± 15.0	74.5 ± 12.8	99.4 ± 0.7
RTI/BMS	0.0 ± 0.0	0.0 ± 0.0	46.2 ± 23.4	95.6 ± 4.4
CBS	0.0 ± 0.0	0.0 ± 0.0	70.3 ± 19.3	100.0 ± 0.1
FLAT	0.0 ± 0.0	0.0 ± 0.0	41.8 ± 34.8	80.2 ± 39.6
SW	0.0 ± 0.0	0.0 ± 0.0	30.2 ± 44.7	38.0 ± 46.9
PLANNING	0.0 ± 0.0	0.0 ± 0.0	9.9 ± 9.9	28.6 ± 28.6
AIS	0.0 ± 0.0	0.0 ± 0.0	29.8 ± 0.0	75.0 ± 0.0
QG	0.0 ± 0.0	0.0 ± 0.0	0.0 ± 0.0	0.0 ± 0.0
BMC	0.0 ± 0.0	0.0 ± 0.0	0.0 ± 0.0	0.0 ± 0.0
DIMACS	0.0 ± 0.0	0.0 ± 0.0	1.4 ± 2.3	27.4 ± 35.9
BEIJING	0.0 ± 0.0	0.0 ± 0.0	14.8 ± 0.0	15.4 ± 0.0

Table 1. Comparative table on SATLIB benchmarks by domain, for two methods: the Product Logic, and the Gödel Trick Uniform. Columns: S is the number of Samples Solved, B is the number of problems solved by keeping the best results among the samples.

A more detailed table that lists the results on every individual benchmark is available in Appendix E. Given that each sample can be run in parallel, we explore multiple initial interpretations efficiently. For each problem, we evaluated 100 samples (equivalent to 100 independent runs) and computed two metrics:  $S$ , the percentage of successfully solved instances across all samples, and  $B$ , the number of solved problems considering the best result among the 100 samples for each problem. Note that each sample is computed in parallel on the GPU, and memory usage remains minimal.

Consequently, the  $B$  measure can be further improved by increasing the number of samples.

### 7.3. Results

The results clearly demonstrate that GT yields a substantial improvement over all baselines, with the Uniform variant achieving the best performance. This trend is consistent across almost all problems, with GT-Uniform always matching or outperforming GT-Logistic. In fact, there was only one instance where the Logistic variant performed better than the Uniform one.

## 8. Visual Sudoku

In addition to SAT problems, we evaluated GT on the Visual Sudoku task (Augustine et al., 2022), a NeSy problem where the goal is to determine whether a given Sudoku grid, represented by MNIST images, is valid. The complete knowledge of Sudoku rules is provided as a logical formula in CNF, and the only available ground truth is whether the Sudoku is valid or not—no direct supervision is provided for the individual digits. During training, we excluded invalid Sudoku instances, as they provide little signal for learning.

The 9x9 variant of this task, which we consider, is particularly challenging. Classical neural networks struggle due to the discrete nature of the logical constraints. Among NeSy approaches, exact probabilistic inference is computationally prohibitive, while fuzzy logic-based methods yield poor results. For instance, LTN (Badreddine et al., 2022) was only tested on the 4x4 variant (Morra et al., 2023).

We compare with an CNN, NeuPSL (Pryor et al., 2022), and A-NeSI (van Krieken et al., 2023).<sup>2</sup> The experiments have been conducted using a machine equipped with an NVIDIA GTX 3070 with 12GB RAM. For the perception neural network, we use the same architecture as A-NeSI, replacing the final softmax layer with a categorical version of the GT described in Appendix C.

Regarding knowledge integration, training was divided into two phases. Initially, we assumed clause independence and applied GT separately to each, which improved convergence. This assumption was later removed to account for clause dependencies. See Appendix F for details.

The results are reported in Table 2, and show comparable accuracy w.r.t. A-NeSI. However, using the same hardware, A-NeSI requires approximately 20 minutes per run, while GT only requires 8 minutes, demonstrating a significant computational advantage.

<sup>2</sup>We use the baseline results reported by (van Krieken et al., 2023). We run A-NeSI on our machine to compare execution time.

Method	Accuracy
CNN	51.20 $\pm$ 2.20
NeuPSL	51.50 $\pm$ 1.37
A-NeSI	62.25 $\pm$ 2.20
GT	62.95 $\pm$ 1.42

Table 2. Comparison of methods on the Visual Sudoku task.

## 9. Conclusions and Future Work

We introduced the Gödel Trick (GT), which enhances optimisation by incorporating controlled noise into the Gödel logic. This noise improves exploration of the solution space, mitigating the tendency of Gödel logic to prematurely converge to local optima.

Our experiments on SAT problems demonstrated that GT significantly outperforms existing fuzzy logic-based approaches. In the Visual Sudoku task, GT matches the performance of SOTA methods while requiring considerably less computational time.

Future work will focus on extending GT with optimisations inspired by the Local Search Algorithm (LSA) literature, for instance with Tabu Search, to further improve convergence and robustness. We will also explore replacing the Gödel logic with alternative LSA-based methods in a NeSy framework, assessing their impact on learning. Additionally, we plan to evaluate GT on more complex NeSy tasks and experiment with alternative noise distributions beyond Logistic and Uniform to understand their effect on performance and generalisation. Finally, we aim to investigate the integration of the Gödel Trick into models capable of learning knowledge, such as DSL (Daniele et al., 2023a), to assess its potential in end-to-end neurosymbolic learning frameworks.

**Limitations** While this paper focuses on optimisation, it does not consider whether the optima found are desirable. NeSy methods might find optima that do not generalise well, as studied under the banner of Reasoning Shortcuts (Marconato et al., 2024b;a). Furthermore, the Gödel trick is limited by the independence assumption in NeSy (van Krieken et al., 2024), which may impact its ability to represent complex dependencies between concepts.

**Acknowledgments** We would like to express our gratitude to Samy Badreddine for the insightful discussions and valuable feedback, which had a significant impact on this work. We also thank Samuel Cognolato and Davide Bizzaro for their helpful comments and suggestions.

## Impact Statement

This paper presents work whose goal is to advance Neurosymbolic integration. There are many potential societal consequences of our work, in particular by encouraging neural networks to adhere to given requirements. We do not believe there are any negative societal consequences we must specifically highlight here.

## References

- Kareem Ahmed, Stefano Teso, Kai-Wei Chang, Guy Van den Broeck, and Antonio Vergari. Semantic probabilistic layers for neuro-symbolic learning. *Advances in Neural Information Processing Systems*, 35:29944–29959, 2022.
- Eriq Augustine, Connor Pryor, Charles Dickens, Jay Pujara, William Wang, and Lise Getoor. Visual sudoku puzzle classification: A suite of collective neuro-symbolic tasks. In *International Workshop on Neural-Symbolic Learning and Reasoning (NeSy)*, 2022.
- Samy Badreddine, Artur d’Avila Garcez, Luciano Serafini, and Michael Spranger. Logic tensor networks. *Artificial Intelligence*, 303:103649, 2022.
- Armin Biere, Marijn Heule, and Hans van Maaren. *Handbook of satisfiability*, volume 185. IOS press, 2009.
- Mark Chavira and Adnan Darwiche. On probabilistic inference by weighted model counting. *Artificial Intelligence*, 172(6-7):772–799, 2008.
- Y Choi, Antonio Vergari, and Guy Van den Broeck. Probabilistic circuits: A unifying framework for tractable probabilistic models. *UCLA*. URL: <http://starai.cs.ucla.edu/papers/ProbCirc20.pdf>, page 6, 2020.
- Alessandro Daniele and Luciano Serafini. Knowledge enhanced neural networks. In *PRICAI 2019: Trends in Artificial Intelligence: 16th Pacific Rim International Conference on Artificial Intelligence, Cuvu, Yanuca Island, Fiji, August 26–30, 2019, Proceedings, Part I 16*, pages 542–554. Springer, 2019.
- Alessandro Daniele, Tommaso Campari, Sagar Malhotra, and Luciano Serafini. Deep symbolic learning: discovering symbols and rules from perceptions. In *Proceedings of the Thirty-Second International Joint Conference on Artificial Intelligence*, pages 3597–3605, 2023a.
- Alessandro Daniele, Emile van Krieken, Luciano Serafini, and Frank van Harmelen. Refining neural network predictions using background knowledge. *Machine Learning*, 112(9):3293–3331, 2023b.
- Lennert De Smet, Emanuele Sansone, and Pedro Zuidberg Dos Martires. Differentiable sampling of categorical distributions using the CatLog-derivative trick. In A. Oh, T. Naumann, A. Globerson, K. Saenko, M. Hardt, and S. Levine, editors, *Advances in Neural Information Processing Systems*, volume 36, pages 30416–30428. Curran Associates, Inc., 2023.
- Michelangelo Diligenti, Marco Gori, and Claudio Sacca. Semantic-based regularization for learning and inference. *Artificial Intelligence*, 244:143–165, 2017.
- Jonathan Feldstein, Paulius Dilkas, Vaishak Belle, and Efthymia Tsamoura. Mapping the neuro-symbolic ai landscape by architectures: A handbook on augmenting deep learning through symbolic reasoning, 2024. URL <https://arxiv.org/abs/2410.22077>.
- Thomas Flinkow, Barak A Pearlmuter, and Rosemary Monahan. Comparing differentiable logics for learning with logical constraints. *arXiv preprint arXiv:2407.03847*, 2024.
- Eleonora Giunchiglia, Alex Tatomir, Mihaela Cătălina Stoian, and Thomas Lukasiewicz. Ccn+: A neuro-symbolic framework for deep learning with requirements. *International Journal of Approximate Reasoning*, page 109124, 2024.
- Mattia Medina Grespan, Ashim Gupta, and Vivek Srikumar. Evaluating relaxations of logic for neural networks: A comprehensive study. *arXiv preprint arXiv:2107.13646*, 2021.
- Emil Julius Gumbel. Statistical theory of extreme value and some practical applications. *Nat. Bur. Standards Appl. Math. Ser.* 33, 1954.
- Madan M Gupta and J11043360726 Qi. Theory of t-norms and fuzzy inference methods. *Fuzzy sets and systems*, 40(3):431–450, 1991.
- Holger H Hoos and Thomas Stützle. Local search algorithms for sat: An empirical evaluation. *Journal of Automated Reasoning*, 24(4):421–481, 2000a.
- Holger H Hoos and Thomas Stützle. Satlib: An online resource for research on sat. *Sat*, 2000:283–292, 2000b.
- Eric Jang, Shixiang Gu, and Ben Poole. Categorical reparameterization with gumbel-softmax. In *International Conference on Learning Representations*, 2022.
- Diederik P. Kingma and Max Welling. Auto-encoding variational bayes. In Yoshua Bengio and Yann LeCun, editors, *2nd International Conference on Learning Representations, ICLR 2014, Banff, AB, Canada, April 14-16, 2014, Conference Track Proceedings*, 2014. URL <http://arxiv.org/abs/1312.6114>.

- Doga Kisa, Guy Van den Broeck, Arthur Choi, and Adnan Darwiche. Probabilistic sentential decision diagrams. In *Fourteenth International Conference on the Principles of Knowledge Representation and Reasoning*, 2014.
- Erich Peter Klement, Radko Mesiar, and Endre Pap. *Triangular norms*, volume 8. Springer Science & Business Media, 2013.
- Jaron Maene, Vincent Derkinderen, and Luc De Raedt. On the hardness of probabilistic neurosymbolic learning. In *Forty-first International Conference on Machine Learning*, 2024.
- Robin Manhaeve, Sebastijan Dumancic, Angelika Kimmig, Thomas Demeester, and Luc De Raedt. Deepprolog: Neural probabilistic logic programming. *Advances in neural information processing systems*, 31, 2018.
- Emanuele Marconato, Samuele Bortolotti, Emile van Krieken, Antonio Vergari, Andrea Passerini, and Stefano Teso. Bears make neuro-symbolic models aware of their reasoning shortcuts. In *The 40th Conference on Uncertainty in Artificial Intelligence*, 2024a.
- Emanuele Marconato, Stefano Teso, Antonio Vergari, and Andrea Passerini. Not all neuro-symbolic concepts are created equal: Analysis and mitigation of reasoning shortcuts. *Advances in Neural Information Processing Systems*, 36, 2024b.
- Giuseppe Marra, Sebastijan Dumančić, Robin Manhaeve, and Luc De Raedt. From statistical relational to neurosymbolic artificial intelligence: A survey. *Artificial Intelligence*, 328:104062, 2024. ISSN 0004-3702. doi: 10.1016/j.artint.2023.104062.
- Shakir Mohamed, Mihaela Rosca, Michael Figurnov, and Andriy Mnih. Monte carlo gradient estimation in machine learning. *Journal of Machine Learning Research*, 21 (132):1–62, 2020.
- Lia Morra, Alberto Azzari, Letizia Bergamasco, Marco Braga, Luigi Capogrosso, Federico Delrio, Giuseppe Di Giacomo, Simone Eirauda, Giorgia Ghione, Rocco Giudice, et al. Designing logic tensor networks for visual sudoku puzzle classification. In *NeSy*, pages 223–232, 2023.
- Connor Pryor, Charles Dickens, Eriq Augustine, Alon Albalak, William Wang, and Lise Getoor. Neupsl: Neural probabilistic soft logic. *arXiv preprint arXiv:2205.14268*, 2022.
- David E Rumelhart, Geoffrey E Hinton, and Ronald J Williams. Learning representations by back-propagating errors. *nature*, 323(6088):533–536, 1986.
- Natalia Slusarz, Ekaterina Komendantskaya, Matthew L Daggitt, Robert Stewart, and Kathrin Stark. Logic of differentiable logics: Towards a uniform semantics of dl. In *Proceedings of 24th International Conference on Logic*, volume 94, pages 473–493, 2023.
- Leslie G Valiant. The complexity of enumeration and reliability problems. *siam Journal on Computing*, 8(3): 410–421, 1979.
- Emile van Krieken, Erman Acar, and Frank van Harmelen. Analyzing differentiable fuzzy logic operators. *Artificial Intelligence*, 302:103602, 2022.
- Emile van Krieken, Thiviyan Thanapalasingam, Jakub Tomczak, Frank Van Harmelen, and Annette Ten Teije. Anesi: A scalable approximate method for probabilistic neurosymbolic inference. *Advances in Neural Information Processing Systems*, 36:24586–24609, 2023.
- Emile van Krieken, Pasquale Minervini, Edoardo Ponti, and Antonio Vergari. On the independence assumption in neurosymbolic learning. In *Forty-first International Conference on Machine Learning*, 2024.
- Jingyi Xu, Zilu Zhang, Tal Friedman, Yitao Liang, and Guy Broeck. A semantic loss function for deep learning with symbolic knowledge. In *International conference on machine learning*, pages 5502–5511. PMLR, 2018.

## A. Proofs

### A.1. Gödel Logic with logits

In the standard Gödel logic, the truth values of formulas are interpreted over the interval  $[0, 1]$ . Formally, the interpretation is defined as follows:

$$\begin{aligned} \mathcal{I}(p) &\in [0, 1], \\ \mathcal{I}(\neg\varphi) &= 1 - \mathcal{I}(\varphi) \\ \mathcal{I}(\varphi \wedge \psi) &= \min(\mathcal{I}(\varphi), \mathcal{I}(\psi)) \\ \mathcal{I}(\varphi \vee \psi) &= \max(\mathcal{I}(\varphi), \mathcal{I}(\psi)) \end{aligned}$$

This framework allows for a fuzzy interpretation of logic, where truth values can range continuously in  $[0, 1]$ .

In our work, we extend these operations to real numbers  $\mathbb{R}$ , working with NN's pre-activations (interpretable as logits in GT) instead of bounded truth values. Since the sigmoid function  $\sigma(x)$  is monotonically increasing, it preserves the relative ordering of the logits, and thus the min and max operations applied to the logits behave consistently with the operations on values in  $[0, 1]$ . For the negation instead we exploit a known property of sigmoid function:  $\sigma(-x) = 1 - \sigma(x)$ . This new variant of Gödel Logic (defined in Section 2.2) is as follows:

$$\begin{aligned} \mathcal{G}(p) &\in \mathbb{R}, \\ \mathcal{G}(\neg\varphi) &= -\mathcal{G}(\varphi), \\ \mathcal{G}(\varphi \wedge \psi) &= \min(\mathcal{G}(\varphi), \mathcal{G}(\psi)), \\ \mathcal{G}(\varphi \vee \psi) &= \max(\mathcal{G}(\varphi), \mathcal{G}(\psi)). \end{aligned}$$

Here we show that  $\mathcal{I}$  and  $\mathcal{G}$  are indeed equivalent. Assuming  $\mathcal{I}(p) = \sigma(\mathcal{G}(p))$ , it holds  $\mathcal{I}(\varphi) = \sigma(\mathcal{G}(\varphi))$  for every formula  $\varphi$ :

1. Negation:  $\sigma(-x) = 1 - \sigma(x)$ , hence applying negation before or after the sigmoid yields the same result.
2. Conjunction:  $\sigma(\min(x, y)) = \min(\sigma(x), \sigma(y))$ , preserving the interpretation of conjunction.
3. Disjunction:  $\sigma(\max(x, y)) = \max(\sigma(x), \sigma(y))$ , preserving the interpretation of disjunction.

Thus, applying Gödel logic to pre-activations is equivalent to applying it to bounded truth values after the sigmoid.

### A.2. Relation between Gödel logic and Boolean logic

**Theorem 4.1.** *Consider a Gödel interpretation  $\mathcal{G}$ . Define the Boolean interpretation  $\mathcal{B}$  obtained by setting  $\mathcal{B}(p) = s(\mathcal{G}(p))$  for all propositional variables  $p \in P$ . Then for all formulas  $\varphi$ , we have  $s(\mathcal{G}(\varphi)) = \mathcal{B}(\varphi)$ .*

*Proof.* Before proceeding with the proof, it is useful to consider a common property regarding all fuzzy logics based on  $t$ -norms and  $t$ -conorms (including Gödel Logic): they represent a generalization of classical logic, i.e., the operators behave as the classical logic counterparts on the extreme values zero and one ( $-1$  and  $+1$  in our modified Gödel Logic on Reals). As such, the classical logic interpretation of Section 2.1 can be redefined as:

$$\begin{aligned} \mathcal{B}(p) &\in \{-1, +1\} \\ \mathcal{B}(\neg\varphi) &= -\mathcal{B}(\varphi) \\ \mathcal{B}(\varphi \wedge \psi) &= \min(\mathcal{B}(\varphi), \mathcal{B}(\psi)) \\ \mathcal{B}(\varphi \vee \psi) &= \max(\mathcal{B}(\varphi), \mathcal{B}(\psi)) \end{aligned}$$

We proceed now with the proof, which is by induction on the structure of the formula. Note that for propositional variables  $p \in P$  we have  $s(\mathcal{G}(p)) = \mathcal{B}(p)$  by definition.

#### Negation:

$$s(\mathcal{G}(\neg\varphi)) = s(-\mathcal{G}(\varphi)) = -s(\mathcal{G}(\varphi)) = -\mathcal{B}(\varphi) = \mathcal{B}(\neg\varphi)$$

This follows directly from the fact that  $s(-x) = -s(x)$  on  $\mathbb{R} \setminus \{0\}$ , and from induction. Note that this would not hold if we assumed zero is a valid truth value.

#### Conjunction:

$$\begin{aligned} s(\mathcal{G}(\varphi \wedge \psi)) &= s(\min(\mathcal{G}(\varphi), \mathcal{G}(\psi))) \\ &= \min(s(\mathcal{G}(\varphi)), s(\mathcal{G}(\psi))) \\ &= \min(\mathcal{B}(\varphi), \mathcal{B}(\psi)) = \mathcal{B}(\varphi \wedge \psi) \end{aligned}$$

The second step follows from the fact that the minimum of two inputs will be negative iff at least one input is negative. Then, we use induction. The case for disjunction is analogous.  $\square$

### A.3. Number of Negations

**Theorem 5.2.** *The partial derivative  $\frac{\partial \varphi}{\partial \psi_i}$ , as calculated along a path  $\mathcal{P} = (\varphi, \psi_1, \dots, p)$ , takes values in  $\{-1, 0, 1\}$ . If different from zero, then the sign of the gradient is positive iff the number of the negations in the path is even:*

$$\frac{\partial \varphi}{\partial \psi_i} = (-1)^n$$

with  $n$  the number of negations in the subpath from  $\varphi$  to  $\psi_i$ .

*Proof.* The value of  $\frac{\partial \varphi}{\partial \psi}$  depends on the chain of partial derivatives computed along the path. The derivatives for the min (and max) operation is 1 if the corresponding subformula is selected as the minimum (maximum), 0 otherwise. The derivative for negation is always  $-1$ . Therefore, each

factor in the chain rule formula is in  $\{-1, 0, 1\}$ , and the entire product will be 0 if any factor is 0. Otherwise, the product will be  $-1$  or  $1$ , depending on whether the number of negations in the path is even or odd.  $\square$

#### A.4. Unique Active Path

**Theorem 5.4.** *Given a formula  $\varphi$ , there exists a unique active path  $\mathcal{P} = (\varphi, \psi_1, \dots, p)$  in the computational graph of  $\varphi$ .*

*Proof.* We proceed by induction on the structure of the formula.

**Base Case (Atomic Proposition):** If  $\varphi = p$ , where  $p$  is an atomic proposition, we have  $\frac{\partial \varphi}{\partial p} = 1$ . There are no intermediate subformulas, so the path is  $\mathcal{P} = (p)$ , and the gradient is trivially 1.

**Inductive Step (Negation):** Suppose the inductive hypothesis holds for a subformula  $\psi$ ; i.e., there exists a unique active path in the computational graph of  $\psi$ . Assume  $\varphi = \neg\psi$ . The gradient of  $\varphi$  with respect to  $p$  is:

$$\frac{\partial \varphi}{\partial p} = \frac{\partial \varphi}{\partial \psi} \cdot \frac{\partial \psi}{\partial p} = -\frac{\partial \psi}{\partial p}.$$

which is different from zero, meaning the path is still active.

**Inductive Step (Conjunction/Disjunction):** Consider the case where  $\varphi = \psi_1 \wedge \psi_2$ . By the inductive hypothesis, we know that there exists a unique active path from each subformula  $\psi_1$  and  $\psi_2$  to their respective atomic propositions  $p_1$  and  $p_2$ , and that the properties hold along these paths.

Since conjunction is interpreted as the minimum function, only the path corresponding to the subformula with the smallest truth value will have a non-zero gradient. Let's assume  $\mathcal{G}(\psi_1) < \mathcal{G}(\psi_2)$ , then the gradient with respect to  $p_1$  is:

$$\frac{\partial \varphi}{\partial p_1} = \frac{\partial \varphi}{\partial \psi_1} \cdot \frac{\partial \psi_1}{\partial p_1} = \frac{\partial \psi_1}{\partial p_1}.$$

and the gradient with respect to  $p_2$  is:

$$\frac{\partial \varphi}{\partial p_2} = \frac{\partial \varphi}{\partial \psi_2} \cdot \frac{\partial \psi_2}{\partial p_2} = 0.$$

If  $\mathcal{G}(\psi_1) > \mathcal{G}(\psi_2)$ , then the gradient with respect to  $p_1$  is zero, while the gradient with respect to  $p_2$  is non-zero. The case for disjunction follows a similar reasoning, with the difference that the maximum function is used.  $\square$

#### A.5. Discrete Derivative

**Theorem 5.5.** *Let  $\varphi$  be a formula, and let  $\pi$  be a subformula in the active path of  $\varphi$ . The partial derivative  $\frac{\partial \varphi}{\partial \pi}$  is equal to the product of the implicit interpretation of the two formulas:*

$$\frac{\partial \varphi}{\partial \pi} = \mathcal{B}(\varphi) \cdot \mathcal{B}(\pi)$$

*Proof.* We proceed by induction on the structure of the formula  $\varphi$ .

**Base Case:** If  $\varphi = \pi$ , then:

$$\begin{aligned} \frac{\partial \varphi}{\partial \pi} &= \frac{\partial \pi}{\partial \pi} = 1 = (\pm 1)^2 \\ &= \mathcal{B}(\varphi)^2 = \mathcal{B}(\varphi) \cdot \mathcal{B}(\pi) \end{aligned}$$

**Inductive Step (Negation):** Consider  $\varphi = \neg\psi$ . Applying the chain rule:

$$\frac{\partial \varphi}{\partial \pi} = \frac{\partial \varphi}{\partial \psi} \cdot \frac{\partial \psi}{\partial \pi} = -\frac{\partial \psi}{\partial \pi} \quad (8)$$

$$= -\mathcal{B}(\psi) \cdot \mathcal{B}(\pi) \quad (9)$$

$$= \mathcal{B}(\varphi) \cdot \mathcal{B}(\pi) \quad (10)$$

where (9) corresponds to the inductive hypothesis, and (10) is a consequence of  $\varphi = \neg\psi$ . Hence, the theorem holds.

**Inductive Step (Conjunction/Disjunction):** Consider  $\varphi = \psi_1 \wedge \psi_2$ . The derivative is non-zero only for the subformula with the smallest truth value. Assume  $\psi_1$ , i.e.

$$\mathcal{G}(\varphi) = \min(\mathcal{G}(\psi_1), \mathcal{G}(\psi_2)) = \mathcal{G}(\psi_1)$$

then, we have:

$$\frac{\partial \varphi}{\partial \pi} = \frac{\partial \varphi}{\partial \psi_1} \cdot \frac{\partial \psi_1}{\partial \pi} = \frac{\partial \psi_1}{\partial \pi} \quad (11)$$

$$= \mathcal{B}(\psi_1) \cdot \mathcal{B}(\pi) = \mathcal{B}(\varphi) \cdot \mathcal{B}(\pi) \quad (12)$$

where (11) holds by the inductive hypothesis, and (12) is a consequence of  $\mathcal{G}(\varphi) = \mathcal{G}(\psi_1)$ .

Similarly, for disjunction, the derivative is non-zero for the subformula with the largest truth value, yielding the same result.  $\square$

#### A.6. Candidate paths in CNF

**Theorem 5.11.** *Let  $\varphi$  be a formula expressed in CNF and  $\mathcal{B}$  a boolean interpretation. Let  $\mathcal{P} = (\varphi, c, l)$  be a path from  $\varphi$  to a literal  $l$ . If clause  $c$  is relevant (i.e., it is not a logical consequence of another clause) and it is not satisfied in  $\mathcal{B}$  ( $\mathcal{B}(c) = -1$ ), then  $\mathcal{P}$  is a candidate path for  $\varphi$  and  $\mathcal{B}$ .*

*Proof.* We need to prove that there exists a representation  $\mathcal{G}$  of  $\mathcal{B}$  such that  $\mathcal{P}$  is an active path in  $\mathcal{G}$ . We proceed by defining a procedure to build such a representation:

1. we start by defining four arbitrary truth values,  $\alpha, \beta, \gamma$ , and  $\delta$ , such that  $\beta < \alpha < \gamma < 0 < \delta$ ;

2. we assign the value  $\alpha$  to  $l$ :  $\mathcal{G}(l) = \alpha < 0$ ;
3. we then assign  $\beta$  to the other literals  $l'$  in  $c$ :  $\mathcal{G}(l') = \beta$ ;
4. then, we assign  $\gamma$  to all the literals  $l'$  (excluding the ones with already a value) appearing in some unsatisfied clause  $c'$ :  $\mathcal{G}(l') = \gamma$ . Note that all the literals must be negative since  $c'$  is unsatisfied;
5. Finally, we assign either  $\delta$  or  $-\delta$  to all the propositions not yet considered consistently with  $\mathcal{B}$ :  $\mathcal{G}(p) = \delta$  if  $\mathcal{B}(p) = 1$ ,  $\mathcal{G}(p) = -\delta$  otherwise.

We need to prove two properties of  $\mathcal{G}$ : first, it must be a representation of  $\mathcal{B}$  ( $\mathcal{B}(\psi) = s(\mathcal{G}(\psi))$ , for all formulas  $\psi$ ); secondly, we need to prove that  $\mathcal{P}$  is an active path for the generated interpretation  $\mathcal{G}$ .

Regarding the first property, steps 1 to 4 of the procedure assign truth values to all literals appearing in at least one unsatisfied clause. If  $l'$  is one such literal, it must be negative (otherwise, the clause would be satisfied):

$$\mathcal{B}(l') = -1 = s(\alpha) = s(\beta) = s(\gamma) = s(\mathcal{G}(l'))$$

Step 5 considers all the remaining propositions, i.e., the propositions that appear exclusively inside satisfied clauses. Since it assigns to them a value consistent with  $\mathcal{B}$ , we can conclude that  $\mathcal{G}$  is a representation for  $\mathcal{B}$ .

At this point, we just need to prove that  $\mathcal{P}$  is an active path in  $\mathcal{G}$ . First, note that the value associated to  $l$  is the largest among the literals in  $c$ :

$$\mathcal{G}(c) = \max(\alpha, \beta) = \alpha$$

Hence, if  $c$  is in the active path, the active path is  $\mathcal{P}$ . For  $c$  to be in the active path, it must hold  $\mathcal{G}(c) \leq \mathcal{G}(c')$ , for all the clause  $c'$ . Since  $c$  is assumed to be relevant, all other unsatisfied clauses must have at least one literal which is not in  $c$ , and such a literal has truth value  $\gamma$ :

$$\mathcal{G}(c') = \gamma > \alpha = \mathcal{G}(c)$$

Hence, the min operator selects the clause  $c$ , and  $\mathcal{P}$  must be the active path.  $\square$

### A.7. Stochastic Gödel Interpretations and Probabilistic Logic

**Theorem 6.2.** *Let  $\varphi$  be a formula defined over some propositions  $p_i$ . Let  $\varphi$  be interpreted under probabilistic logic, with  $\pi_i$  the probability associated with proposition  $p_i$ , and let  $\epsilon$  be a continuous distribution over the real numbers.*

*If we define the proposition's truth values as  $\mathcal{G}(p_i) = \theta_\epsilon^{-1}(\pi_i)$ , then:*

$$P(\mathcal{B}_\epsilon(\varphi)) = P(\varphi)$$

*where  $P(\varphi)$  is the probability of  $\varphi$  being true under the probabilistic interpretation.*

*Proof.* We first consider the probability of  $\mathcal{B}_\epsilon(\varphi)$  being positive. Such a probability can be defined as the expected value of the formula's truth value, assuming it to be in  $\{0, 1\}$  rather than  $\{-1, 1\}$ :

$$P(\mathcal{B}_\epsilon(\varphi)) = \mathbb{E}_\epsilon[H(\mathcal{B}_\epsilon(\varphi))] \quad (13)$$

$$= \mathbb{E}_\epsilon[H(s(\mathcal{G}(\varphi; \boldsymbol{\mu})))] \quad (14)$$

where  $H$  is the Heaviside function,  $\mathcal{G}(\varphi; \boldsymbol{\mu})$  is the Gödel interpretation of  $\varphi$  (as defined in 2.2) assuming  $\mathcal{G}(p_i) = \mu_i$ ,  $\epsilon$  is the vector of sampled noise for each proposition, and  $\boldsymbol{\mu}$  is the corresponding vector of noisy interpretations:

$$\mu_i = \mathcal{G}_\epsilon(p_i) = \mathcal{G}(p_i) + \epsilon_i$$

By applying Theorem 4.1:

$$P(\mathcal{B}_\epsilon(\varphi)) = \mathbb{E}_\epsilon[H(s(\mathcal{G}(\varphi; \boldsymbol{\mu})))] \quad (15)$$

$$= \mathbb{E}_\epsilon[H(\mathcal{B}(\varphi; s(\boldsymbol{\mu})))] \quad (16)$$

$$= \mathbb{E}_\gamma[H(\mathcal{B}(\varphi; \boldsymbol{\gamma}))] \quad (17)$$

where in (17) we applied a change of variable on the expectation by defining  $\gamma_i = s(\mu_i)$ . Note that  $\gamma \in \{-1, 1\}^n$ , and the expected value can be represented as a summation:

$$P(\mathcal{B}_\epsilon(\varphi)) = \sum_{\gamma \in \{-1, 1\}^n} H(\mathcal{B}(\varphi; \boldsymbol{\gamma})) P(\boldsymbol{\gamma}) \quad (18)$$

with

$$P(\boldsymbol{\gamma}) = \prod_{i=1}^n P(\gamma_i)^{H(\gamma_i)} (1 - P(\gamma_i))^{1-H(\gamma_i)} \quad (19)$$

Equations (19) and (4) are identical, except for the usage of  $P(\gamma_i)$  instead of  $\pi_i$ . We need to prove the equivalence between these two probabilities:

$$P(\gamma_i) = P(s(\mu_i)) \quad (20)$$

$$= P(\mathcal{G}(p_i) + \epsilon_i > 0) \quad (21)$$

$$= \theta_\epsilon(\mathcal{G}(p_i)) \quad (22)$$

$$= \theta_\epsilon(\theta_\epsilon^{-1}(\pi_i)) = \pi_i \quad (23)$$

where (21) is obtained by applying the definition of  $\mu_i$ , (22) derives from (2), and (23) comes from the definition of  $\mathcal{G}(p_i)$  in theorem statement.

As a consequence,  $P(\boldsymbol{\gamma})$  and  $P(\boldsymbol{\omega})$  of equations (18) and (3) are identical. Therefore:

$$P(\mathcal{B}_\epsilon(\varphi)) = \sum_{\gamma \in \{-1, 1\}^n} H(\mathcal{B}(\varphi; \boldsymbol{\gamma})) P(\boldsymbol{\gamma}) \quad (24)$$

$$= \sum_{\boldsymbol{\omega} \in \{-1, 1\}^n} H(\mathcal{B}(\varphi; \boldsymbol{\omega})) P(\boldsymbol{\omega}) = P(\varphi) \quad (25)$$

$\square$

## B. Example of candidate paths

*Example 4.* Consider the boolean interpretation  $\mathcal{B}$  of Figure 3 for formula  $\varphi = \neg(A \vee B) \wedge (B \vee C) \wedge (C \vee D)$ , and the path  $\mathcal{P}$  that reaches  $A$ :

$$\mathcal{P} = (\varphi, \neg(A \vee B), A \vee B, A)$$

Note that  $\mathcal{B}(A) = -1$  and  $\mathcal{B}(\varphi) = -1$ , while the number of negations is 1. Hence,

$$\mathcal{B}(A) \cdot \mathcal{B}(\varphi) = 1 \neq -1 = (-1)^1$$

For theorem 5.8, we can conclude that the path cannot be active (not a candidate path). Indeed, the same conclusion can be reached thinking it in terms of the continuous representations of  $\mathcal{B}$ : for all possible representations  $\mathcal{G}$  of  $\mathcal{B}$ ,  $\mathcal{G}(A) < 0$  since  $\mathcal{B}(A) = -1$ . Similarly,  $\mathcal{G}(B) > 0$ . As a consequence, the maximum between the two will always be  $\mathcal{G}(B)$ , for all representations  $\mathcal{G}$  of  $\mathcal{B}$ :

$$\mathcal{G}(A \vee B) = \max(\mathcal{G}(A), \mathcal{G}(B)) = \mathcal{G}(B)$$

*Example 5.* Consider the formula  $\varphi = (A \vee B \vee C) \wedge (A \vee B)$  and the path leading to  $\mathcal{G}(C)$ . This path is inactive for all possible interpretations: indeed, the interpretation of the first clause  $\mathcal{G}(A \vee B \vee C) = \max(\mathcal{G}(A), \mathcal{G}(B), \mathcal{G}(C))$  is equal to  $\mathcal{G}(C)$  only if  $C$  has the largest truth value. However, if it is the largest, then the value of the first clause is higher than the second one:

$$\mathcal{G}(A \vee B \vee C) \geq \mathcal{G}(A \vee B)$$

and the interpretation of formula  $\varphi$  becomes

$$\mathcal{G}(\varphi) = \min(\mathcal{G}(A \vee B \vee C), \mathcal{G}(A \vee B)) = \mathcal{G}(A \vee B).$$

As a consequence,  $C$  will never be selected. It is worth noting that the clause containing  $C$  is a logical consequence of the other clause and the value associated to  $C$  is always irrelevant for the interpretation of formula  $\varphi$ .

## C. Gödel Trick with Categorical variables

The Gödel Trick proposed in the Section 6 is defined exclusively on boolean variables. Despite its generality, in the context of NeSy, categorical variables are frequently used (see as an example Section 8), for which the Gödel Trick is not directly applicable. Let  $\pi_i$ , with  $i \in [1, \dots, K]$ , be the probabilities associated with  $K$  categories, such that  $\sum_{i=1}^K \pi_i = 1$ . We can define a propositional variable  $p_i$  for each category, and use the Gödel Trick:  $\mathcal{G}(p_i) = \theta_\epsilon^{-1}(\pi_i)$ . However, by doing so we are implicitly assuming independence between the propositions. On the contrary, we need to assure that exactly one category is true. To include such a constraint, a possibility is to enforce the satisfaction of the

XOR between the  $K$  propositions through logical constraints. However, such a solution could require to include a large amount of rules, reducing the efficiency of the method.

We propose a different strategy (see Section 8 for an empirical evaluation): we define a shift function that shifts the perturbed truth values  $\mathcal{G}_\epsilon(p_i)$  of propositions  $p_i$  in order to enforce the aforementioned constraint:

$$\text{shift}(\mathbf{x}) = \mathbf{x} - \frac{x_i + x_j}{2},$$

where  $i$  and  $j$  are the indexes of the highest and second highest elements of the vector  $\mathbf{x}$ , respectively. Note that for any vector  $\mathbf{x}$ , the shifted vector  $\bar{\mathbf{x}} = \text{shift}(\mathbf{x})$  contains exactly one value larger than zero:

$$\bar{x}_i = x_i - \frac{x_i + x_j}{2} = \frac{x_i - x_j}{2} > 0 \quad (26)$$

$$\bar{x}_j = x_j - \frac{x_i + x_j}{2} = \frac{x_j - x_i}{2} < 0 \quad (27)$$

$$\bar{x}_k \leq \bar{x}_j < 0 \quad \forall k \neq i \quad (28)$$

It is worth to note two properties of the shifted vector: first, the highest element of  $\bar{\mathbf{x}}$  is the only one higher than zero; second, the second-highest element is the negation of the first:  $\bar{x}_j = -\bar{x}_i$ .

We define the vector  $\mathcal{G}_\epsilon(\mathbf{p})$  of perturbed truth values as:

$$\mathcal{G}_\epsilon(\mathbf{p}) = \langle \mathcal{G}_\epsilon(p_1), \mathcal{G}_\epsilon(p_2) \dots \mathcal{G}_\epsilon(p_K) \rangle$$

We also define its shifted version as:  $\bar{\mathcal{G}}_\epsilon(\mathbf{p}) = \text{shift}(\mathcal{G}_\epsilon(\mathbf{p}))$ . Because of the properties of the shift function, we have:  $\bar{\mathcal{G}}_\epsilon(p_i) > 0$  for the highest value  $i$  in  $\mathcal{G}_\epsilon(\mathbf{p})$ , and  $\forall k \neq i \quad \bar{\mathcal{G}}_\epsilon(p_k) < 0$ . As a consequence, the constraint of the categorical variable is satisfied (i.e., only one value is true). Since the shifted truth values are still used in combination with Gödel Logic:

$$\bar{\mathcal{G}}_\epsilon(p_i) = -\bar{\mathcal{G}}_\epsilon(p_j) = \bar{\mathcal{G}}_\epsilon(\neg p_i) \quad (29)$$

representing the categorical variable as a Bernoulli variable that select one among the two highest values.

Finally, when using the Gumbel distribution to generate noise, the resulting behavior is equivalent to the one of the Gumbel-Max Trick (see Appendix D).

## D. Connections with Gumbel-Max Trick

The Gumbel-Max Trick is a well-known reparameterization approach for sampling from a categorical distribution (Gumbel, 1954; Jang et al., 2022). Given a categorical distribution defined by probabilities  $\pi_i$ , the trick allows for an efficient way to sample from this distribution by adding continuous noise to its logits.

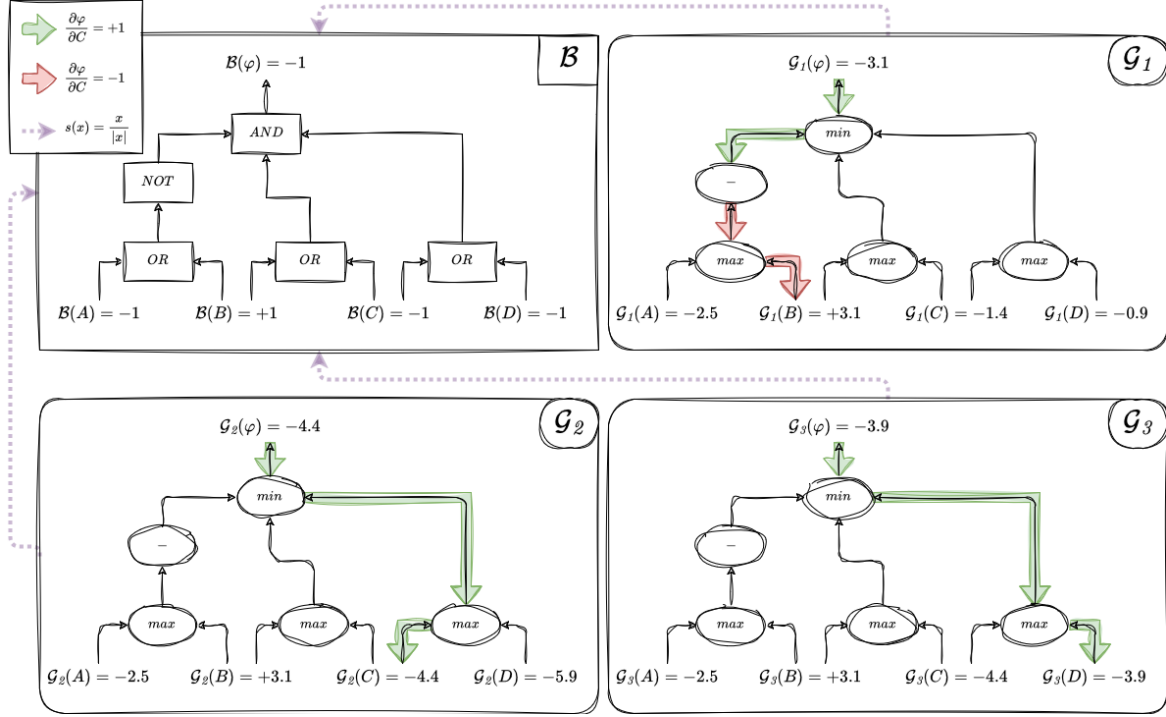


Figure 3. A boolean interpretation  $\mathcal{B}$  (top-left) for the formula  $\varphi = \neg(A \vee B) \wedge (B \vee C) \wedge (C \vee D)$  and three Gödel interpretations ( $\mathcal{G}_1$ ,  $\mathcal{G}_2$ , and  $\mathcal{G}_3$ ) that maps to  $\mathcal{B}$ . Each continuous interpretations have a different active path, leading to a different new version of  $\mathcal{B}$ .

Starting from the softmax logits  $\mathbf{z} = \langle z_1, z_2 \dots z_K \rangle$  of the probabilities  $\pi_i$ , one can add noise sampled from a standard Gumbel distribution to the logits, and the distribution of the argmax of the resulting vector corresponds to the original categorical distribution. Consider the following equation:

$$\mathbf{x} = \text{onehot}(\arg \max_i (z_i + \epsilon_i)) \quad (30)$$

with  $\epsilon_i \sim \text{Gumbel}(0, 1)$ . The key aspect of the Gumbel-Max Trick is that the probability that  $\arg \max_i (z_i + \epsilon_i) = j$  is equivalent to  $\pi_j$ .

Now, consider replacing the  $\arg \max$  function with the shift function, and applying the sign function  $s$  to the resulting vector:

$$\mathbf{v} = s(\text{shift}(\langle z_i + \epsilon_i \rangle)) \quad (31)$$

with the noise still being sampled from a standard Gumbel distribution. As proven in section C, the shift function translates the values of the vector in such a way that only the highest is greater than zero. As a consequence, the sign function  $s$  maps all the values to  $-1$ , except for the  $\arg \max$ , which is mapped to  $+1$ .

Note that, in our framework, we defined  $\top$  to be  $+1$ , and  $\perp$  to be  $-1$ , different from the context of the Gumbel-Max Trick, where  $\perp$  is defined as  $0$ . Therefore, vector  $\mathbf{v}$  can be seen as a rescaled version of  $\mathbf{z}$  suitable for the application

of the Gödel Trick:

$$\mathbf{v} = 2\mathbf{z} - 1 \quad (32)$$

## E. SAT benchmarks results

Results for the entire set of benchmarks are reported in Tables 3 and 4.

## F. Training Phases and Knowledge Integration

To effectively integrate logical knowledge in the Visual Sudoku experiments (Section 8), training was structured into two phases. In the first phase, we treated each logical clause as independent and applied the Gödel Trick (GT) separately to each. This means that, instead of aggregating clause truth values using the  $\min$  function, the model directly outputs the individual truth values of each clause.

In both phases, we used a binary cross-entropy (BCE) loss with target values set to 1. Indeed, since all Sudoku instances in the dataset are valid, every logical clause must be satisfied. The only difference between the two phases is the structure of the loss computation:

- **Phase 1 (Independent Clauses):** The model outputs a matrix where each row corresponds to a sample, and each column corresponds to a clause. The BCE loss is

computed element-wise against a target matrix of the same shape, filled with ones.

- **Phase 2 (Full Dependency):** The model aggregates clause satisfaction using min, producing a single truth value per sample. The BCE loss is then computed on this vector output against a target value of 1 for each sample.

This phased approach helps improve convergence by mitigating the sparsity of gradients introduced by the min operation. In the first phase, optimizing individual clauses separately allows for more stable gradient updates, whereas in the second phase, the full logical dependencies are incorporated.

Empirically, we found that this strategy improves early convergence while still enabling the model to capture the full logical structure in later stages.

Escaping Local Minima in Neurosymbolic Local Search

Benchmark	Product Logic		Godel Logic		GT Uniform		GT Logistic	
	S(%)	B(%)	S(%)	B(%)	S(%)	B(%)	S(%)	B(%)
Uniform Random 3-SAT								
uf20-91	23.8 ± 35.1	48.1 ± 50.0	7.6 ± 6.9	94.9 ± 22.0	<b>99.4 ± 3.1</b>	<b>100.0 ± 0.0</b>	82.4 ± 27.1	99.9 ± 3.2
uf50-218	1.8 ± 9.4	10.0 ± 30.0	0.1 ± 0.4	7.6 ± 26.5	<b>88.7 ± 17.0</b>	<b>100.0 ± 0.0</b>	53.1 ± 40.4	86.8 ± 33.8
uf75-325	0.2 ± 2.3	1.0 ± 9.9	0.0 ± 0.1	1.0 ± 9.9	<b>76.1 ± 23.7</b>	<b>100.0 ± 0.0</b>	38.9 ± 37.1	80.0 ± 40.0
uf100-430	0.0 ± 0.0	0.0 ± 0.0	0.0 ± 0.0	0.1 ± 3.2	<b>69.3 ± 26.1</b>	<b>100.0 ± 0.0</b>	5.8 ± 18.4	21.8 ± 41.3
uf125-538	0.0 ± 0.0	0.0 ± 0.0	0.0 ± 0.0	0.0 ± 0.0	<b>57.5 ± 28.5</b>	<b>100.0 ± 0.0</b>	15.0 ± 26.0	50.0 ± 50.0
uf150-645	0.0 ± 0.0	0.0 ± 0.0	0.0 ± 0.0	0.0 ± 0.0	<b>56.2 ± 29.9</b>	<b>99.0 ± 9.9</b>	7.1 ± 18.7	37.0 ± 48.3
uf200-860	0.0 ± 0.0	0.0 ± 0.0	0.0 ± 0.0	0.0 ± 0.0	<b>74.0 ± 30.6</b>	<b>98.0 ± 14.0</b>	6.4 ± 11.7	48.0 ± 50.0
uf225-960	0.0 ± 0.0	0.0 ± 0.0	0.0 ± 0.0	0.0 ± 0.0	<b>75.6 ± 32.7</b>	<b>99.0 ± 9.9</b>	10.7 ± 21.3	54.0 ± 49.8
uf250-1065	0.0 ± 0.0	0.0 ± 0.0	0.0 ± 0.0	0.0 ± 0.0	<b>73.8 ± 30.1</b>	<b>99.0 ± 9.9</b>	6.0 ± 13.2	40.0 ± 49.0
Random-3-SAT Instances and Backbone-minimal Sub-instances								
RTL_k3_n100_m429	0.0 ± 0.0	0.0 ± 0.0	0.0 ± 0.0	0.0 ± 0.0	<b>69.7 ± 26.0</b>	<b>100.0 ± 0.0</b>	12.5 ± 26.5	40.6 ± 49.1
BMS_k3_n100_m429	0.0 ± 0.0	0.0 ± 0.0	0.0 ± 0.0	0.0 ± 0.0	<b>22.8 ± 27.5</b>	<b>91.2 ± 28.3</b>	4.1 ± 15.5	16.0 ± 36.7
Random 3-SAT Controlled Backbone								
CBS_k3_n100_m403_b10	0.0 ± 0.0	0.0 ± 0.0	0.0 ± 0.0	0.0 ± 0.0	<b>89.8 ± 11.2</b>	<b>100.0 ± 0.0</b>	12.5 ± 24.7	50.5 ± 50.0
CBS_k3_n100_m403_b30	0.0 ± 0.0	0.0 ± 0.0	0.0 ± 0.0	0.0 ± 0.0	<b>73.1 ± 18.4</b>	<b>100.0 ± 0.0</b>	2.0 ± 8.8	18.6 ± 38.9
CBS_k3_n100_m403_b50	0.0 ± 0.0	0.0 ± 0.0	0.0 ± 0.0	0.0 ± 0.0	<b>57.9 ± 21.3</b>	<b>100.0 ± 0.0</b>	0.5 ± 4.0	8.0 ± 27.1
CBS_k3_n100_m403_b70	0.0 ± 0.0	0.0 ± 0.0	0.0 ± 0.0	0.0 ± 0.0	<b>52.4 ± 20.4</b>	<b>100.0 ± 0.0</b>	0.2 ± 1.7	3.4 ± 18.1
CBS_k3_n100_m403_b90	0.0 ± 0.0	0.0 ± 0.0	0.0 ± 0.0	0.0 ± 0.0	<b>27.2 ± 16.6</b>	<b>99.8 ± 4.5</b>	0.0 ± 0.0	0.1 ± 3.2
CBS_k3_n100_m411_b10	0.0 ± 0.0	0.0 ± 0.0	0.0 ± 0.0	0.0 ± 0.0	<b>90.9 ± 10.7</b>	<b>100.0 ± 0.0</b>	14.0 ± 25.5	53.6 ± 49.9
CBS_k3_n100_m411_b30	0.0 ± 0.0	0.0 ± 0.0	0.0 ± 0.0	0.0 ± 0.0	<b>76.2 ± 17.8</b>	<b>100.0 ± 0.0</b>	3.0 ± 11.0	22.3 ± 41.6
CBS_k3_n100_m411_b50	0.0 ± 0.0	0.0 ± 0.0	0.0 ± 0.0	0.0 ± 0.0	<b>62.4 ± 22.1</b>	<b>100.0 ± 0.0</b>	0.8 ± 4.7	10.7 ± 30.9
CBS_k3_n100_m411_b70	0.0 ± 0.0	0.0 ± 0.0	0.0 ± 0.0	0.0 ± 0.0	<b>55.6 ± 21.4</b>	<b>100.0 ± 0.0</b>	0.3 ± 2.3	4.9 ± 21.6
CBS_k3_n100_m411_b90	0.0 ± 0.0	0.0 ± 0.0	0.0 ± 0.0	0.0 ± 0.0	<b>30.2 ± 18.4</b>	<b>99.6 ± 6.3</b>	0.0 ± 0.0	0.0 ± 0.0
CBS_k3_n100_m418_b10	0.0 ± 0.0	0.0 ± 0.0	0.0 ± 0.0	0.0 ± 0.0	<b>92.7 ± 9.1</b>	<b>100.0 ± 0.0</b>	18.2 ± 29.4	59.5 ± 49.1
CBS_k3_n100_m418_b30	0.0 ± 0.0	0.0 ± 0.0	0.0 ± 0.0	0.0 ± 0.0	<b>78.8 ± 17.0</b>	<b>100.0 ± 0.0</b>	3.0 ± 10.4	25.0 ± 43.3
CBS_k3_n100_m418_b50	0.0 ± 0.0	0.0 ± 0.0	0.0 ± 0.0	0.0 ± 0.0	<b>65.7 ± 21.1</b>	<b>100.0 ± 0.0</b>	0.9 ± 5.6	11.1 ± 31.4
CBS_k3_n100_m418_b70	0.0 ± 0.0	0.0 ± 0.0	0.0 ± 0.0	0.0 ± 0.0	<b>60.9 ± 21.4</b>	<b>100.0 ± 0.0</b>	0.3 ± 2.5	6.2 ± 24.1
CBS_k3_n100_m418_b90	0.0 ± 0.0	0.0 ± 0.0	0.0 ± 0.0	0.0 ± 0.0	<b>34.7 ± 20.0</b>	<b>100.0 ± 0.0</b>	0.0 ± 0.0	0.1 ± 3.2
CBS_k3_n100_m423_b10	0.0 ± 0.0	0.0 ± 0.0	0.0 ± 0.0	0.0 ± 0.0	<b>93.6 ± 9.0</b>	<b>100.0 ± 0.0</b>	21.0 ± 30.8	65.9 ± 47.4
CBS_k3_n100_m423_b30	0.0 ± 0.0	0.0 ± 0.0	0.0 ± 0.0	0.0 ± 0.0	<b>81.9 ± 16.2</b>	<b>100.0 ± 0.0</b>	4.7 ± 15.0	31.1 ± 46.3
CBS_k3_n100_m423_b50	0.0 ± 0.0	0.0 ± 0.0	0.0 ± 0.0	0.0 ± 0.0	<b>69.6 ± 20.8</b>	<b>100.0 ± 0.0</b>	1.3 ± 6.4	12.9 ± 33.5
CBS_k3_n100_m423_b70	0.0 ± 0.0	0.0 ± 0.0	0.0 ± 0.0	0.0 ± 0.0	<b>63.9 ± 21.1</b>	<b>100.0 ± 0.0</b>	0.3 ± 2.2	6.2 ± 24.1
CBS_k3_n100_m423_b90	0.0 ± 0.0	0.0 ± 0.0	0.0 ± 0.0	0.0 ± 0.0	<b>38.0 ± 20.7</b>	<b>99.9 ± 3.2</b>	0.0 ± 0.0	0.1 ± 3.2
CBS_k3_n100_m429_b10	0.0 ± 0.0	0.0 ± 0.0	0.0 ± 0.0	0.0 ± 0.0	<b>94.7 ± 8.0</b>	<b>100.0 ± 0.0</b>	26.6 ± 33.6	71.3 ± 45.2
CBS_k3_n100_m429_b30	0.0 ± 0.0	0.0 ± 0.0	0.0 ± 0.0	0.0 ± 0.0	<b>83.0 ± 16.0</b>	<b>100.0 ± 0.0</b>	6.4 ± 17.1	34.3 ± 47.5
CBS_k3_n100_m429_b50	0.0 ± 0.0	0.0 ± 0.0	0.0 ± 0.0	0.0 ± 0.0	<b>71.6 ± 20.8</b>	<b>100.0 ± 0.0</b>	1.6 ± 7.8	15.3 ± 36.0
CBS_k3_n100_m429_b70	0.0 ± 0.0	0.0 ± 0.0	0.0 ± 0.0	0.0 ± 0.0	<b>67.1 ± 20.5</b>	<b>100.0 ± 0.0</b>	0.5 ± 3.6	8.6 ± 28.0
CBS_k3_n100_m429_b90	0.0 ± 0.0	0.0 ± 0.0	0.0 ± 0.0	0.0 ± 0.0	<b>41.2 ± 22.3</b>	<b>100.0 ± 0.0</b>	0.0 ± 0.0	0.1 ± 3.2
CBS_k3_n100_m435_b10	0.0 ± 0.0	0.0 ± 0.0	0.0 ± 0.0	0.0 ± 0.0	<b>95.5 ± 7.0</b>	<b>100.0 ± 0.0</b>	31.7 ± 36.2	74.3 ± 43.7
CBS_k3_n100_m435_b30	0.0 ± 0.0	0.0 ± 0.0	0.0 ± 0.0	0.0 ± 0.0	<b>85.0 ± 15.2</b>	<b>100.0 ± 0.0</b>	7.3 ± 18.1	37.7 ± 48.5
CBS_k3_n100_m435_b50	0.0 ± 0.0	0.0 ± 0.0	0.0 ± 0.0	0.0 ± 0.0	<b>75.1 ± 19.4</b>	<b>100.0 ± 0.0</b>	1.9 ± 8.0	17.8 ± 38.3
CBS_k3_n100_m435_b70	0.0 ± 0.0	0.0 ± 0.0	0.0 ± 0.0	0.0 ± 0.0	<b>70.7 ± 19.3</b>	<b>100.0 ± 0.0</b>	0.6 ± 3.4	10.5 ± 30.7
CBS_k3_n100_m435_b90	0.0 ± 0.0	0.0 ± 0.0	0.0 ± 0.0	0.0 ± 0.0	<b>45.2 ± 22.8</b>	<b>99.9 ± 3.2</b>	0.0 ± 0.1	0.2 ± 4.5
CBS_k3_n100_m441_b10	0.0 ± 0.0	0.0 ± 0.0	0.0 ± 0.0	0.0 ± 0.0	<b>96.6 ± 5.7</b>	<b>100.0 ± 0.0</b>	34.8 ± 37.4	80.7 ± 39.5
CBS_k3_n100_m441_b30	0.0 ± 0.0	0.0 ± 0.0	0.0 ± 0.0	0.0 ± 0.0	<b>87.5 ± 13.7</b>	<b>100.0 ± 0.0</b>	10.8 ± 23.0	45.1 ± 49.8
CBS_k3_n100_m441_b50	0.0 ± 0.0	0.0 ± 0.0	0.0 ± 0.0	0.0 ± 0.0	<b>77.8 ± 19.1</b>	<b>100.0 ± 0.0</b>	2.2 ± 9.3	21.1 ± 40.8
CBS_k3_n100_m441_b70	0.0 ± 0.0	0.0 ± 0.0	0.0 ± 0.0	0.0 ± 0.0	<b>72.1 ± 20.0</b>	<b>100.0 ± 0.0</b>	0.6 ± 3.3	10.1 ± 30.1
CBS_k3_n100_m441_b90	0.0 ± 0.0	0.0 ± 0.0	0.0 ± 0.0	0.0 ± 0.0	<b>49.8 ± 23.0</b>	<b>100.0 ± 0.0</b>	0.0 ± 0.1	0.3 ± 5.5
CBS_k3_n100_m449_b10	0.0 ± 0.0	0.0 ± 0.0	0.0 ± 0.0	0.0 ± 0.0	<b>97.5 ± 5.3</b>	<b>100.0 ± 0.0</b>	42.5 ± 39.1	83.6 ± 37.0
CBS_k3_n100_m449_b30	0.0 ± 0.0	0.0 ± 0.0	0.0 ± 0.0	0.0 ± 0.0	<b>90.0 ± 12.6</b>	<b>100.0 ± 0.0</b>	13.1 ± 25.3	50.6 ± 50.0
CBS_k3_n100_m449_b50	0.0 ± 0.0	0.0 ± 0.0	0.0 ± 0.0	0.0 ± 0.0	<b>81.0 ± 18.0</b>	<b>100.0 ± 0.0</b>	3.2 ± 11.5	25.0 ± 43.3
CBS_k3_n100_m449_b70	0.0 ± 0.0	0.0 ± 0.0	0.0 ± 0.0	0.0 ± 0.0	<b>77.6 ± 18.8</b>	<b>100.0 ± 0.0</b>	1.3 ± 6.9	15.0 ± 35.7
CBS_k3_n100_m449_b90	0.0 ± 0.0	0.0 ± 0.0	0.0 ± 0.0	0.0 ± 0.0	<b>55.8 ± 23.8</b>	<b>100.0 ± 0.0</b>	0.0 ± 0.2	0.8 ± 8.9

Table 3. Comparative table showing results on SATLIB benchmarks for four methods. The table continues on the next page.

Escaping Local Minima in Neurosymbolic Local Search

Benchmark	Product Logic		Godel Logic		GT Uniform		GT Logistic	
	S(%)	B(%)	S(%)	B(%)	S(%)	B(%)	S(%)	B(%)
Flat Graph Colouring								
flat30-60	0.0 ± 0.0	0.0 ± 0.0	0.1 ± 0.2	6.0 ± 23.7	<b>96.6 ± 10.0</b>	<b>100.0 ± 0.0</b>	26.8 ± 12.8	<b>100.0 ± 0.0</b>
flat50-115	0.0 ± 0.0	0.0 ± 0.0	0.0 ± 0.0	0.0 ± 0.0	<b>64.7 ± 19.1</b>	<b>100.0 ± 0.0</b>	0.0 ± 0.1	0.3 ± 5.5
flat75-180	0.0 ± 0.0	0.0 ± 0.0	0.0 ± 0.0	0.0 ± 0.0	<b>32.7 ± 16.0</b>	<b>100.0 ± 0.0</b>	0.0 ± 0.1	1.0 ± 9.9
flat100-239	0.0 ± 0.0	0.0 ± 0.0	0.0 ± 0.0	0.0 ± 0.0	<b>15.2 ± 10.7</b>	<b>100.0 ± 0.0</b>	0.0 ± 0.0	0.0 ± 0.0
flat200-479	0.0 ± 0.0	0.0 ± 0.0	0.0 ± 0.0	0.0 ± 0.0	<b>0.0 ± 0.1</b>	<b>1.0 ± 9.9</b>	0.0 ± 0.0	0.0 ± 0.0
Morphed Graph Colouring								
SW100-8-2	0.0 ± 0.0	0.0 ± 0.0	0.0 ± 0.0	0.0 ± 0.0	<b>95.2 ± 7.8</b>	<b>100.0 ± 0.0</b>	0.0 ± 0.0	0.0 ± 0.0
SW100-8-3	0.0 ± 0.0	0.0 ± 0.0	0.0 ± 0.0	0.0 ± 0.0	<b>7.4 ± 9.9</b>	<b>80.0 ± 40.0</b>	0.0 ± 0.0	0.0 ± 0.0
SW100-8-4	0.0 ± 0.0	0.0 ± 0.0	0.0 ± 0.0	0.0 ± 0.0	0.0 ± 0.0	0.0 ± 0.0	0.0 ± 0.0	0.0 ± 0.0
SW100-8-5	0.0 ± 0.0	0.0 ± 0.0	0.0 ± 0.0	0.0 ± 0.0	0.0 ± 0.0	0.0 ± 0.0	0.0 ± 0.0	0.0 ± 0.0
SW100-8-6	0.0 ± 0.0	0.0 ± 0.0	0.0 ± 0.0	0.0 ± 0.0	0.0 ± 0.0	0.0 ± 0.0	0.0 ± 0.0	0.0 ± 0.0
SW100-8-7	0.0 ± 0.0	0.0 ± 0.0	0.0 ± 0.0	0.0 ± 0.0	0.0 ± 0.0	0.0 ± 0.0	0.0 ± 0.0	0.0 ± 0.0
SW100-8-8	0.0 ± 0.0	0.0 ± 0.0	0.0 ± 0.0	0.0 ± 0.0	0.0 ± 0.0	0.0 ± 0.0	0.0 ± 0.0	0.0 ± 0.0
SW100-8-p0	0.0 ± 0.0	0.0 ± 0.0	0.0 ± 0.0	0.0 ± 0.0	0.0 ± 0.0	0.0 ± 0.0	0.0 ± 0.0	0.0 ± 0.0
sw100-8-lp0-c5	0.0 ± 0.0	0.0 ± 0.0	0.0 ± 0.0	0.0 ± 0.0	<b>100.0 ± 0.1</b>	<b>100.0 ± 0.0</b>	0.0 ± 0.0	0.0 ± 0.0
sw100-8-lp1-c5	0.0 ± 0.0	0.0 ± 0.0	0.0 ± 0.0	0.0 ± 0.0	<b>99.9 ± 0.4</b>	<b>100.0 ± 0.0</b>	0.0 ± 0.0	0.0 ± 0.0
Planning								
blocksworld	0.0 ± 0.0	0.0 ± 0.0	0.0 ± 0.0	0.0 ± 0.0	<b>19.9 ± 22.6</b>	<b>57.1 ± 49.5</b>	13.6 ± 21.0	42.9 ± 49.5
logistics	0.0 ± 0.0	0.0 ± 0.0	0.0 ± 0.0	0.0 ± 0.0	0.0 ± 0.0	0.0 ± 0.0	0.0 ± 0.0	0.0 ± 0.0
All interval series								
ais	0.0 ± 0.0	0.0 ± 0.0	0.0 ± 0.0	0.0 ± 0.0	<b>29.8 ± 41.2</b>	<b>75.0 ± 43.3</b>	0.8 ± 1.3	25.0 ± 43.3
Quasigroup								
QG	0.0 ± 0.0	0.0 ± 0.0	0.0 ± 0.0	0.0 ± 0.0	0.0 ± 0.0	0.0 ± 0.0	<b>0.4 ± 1.2</b>	<b>10.0 ± 30.0</b>
Bounded model checking								
bmc	0.0 ± 0.0	0.0 ± 0.0	0.0 ± 0.0	0.0 ± 0.0	0.0 ± 0.0	0.0 ± 0.0	0.0 ± 0.0	0.0 ± 0.0
DIMACS								
ai	0.0 ± 0.0	0.0 ± 0.0	0.0 ± 0.0	0.0 ± 0.0	<b>6.4 ± 6.4</b>	<b>93.0 ± 25.5</b>	0.0 ± 0.0	0.0 ± 0.0
ai2	0.0 ± 0.0	0.0 ± 0.0	0.0 ± 0.0	0.0 ± 0.0	<b>1.6 ± 2.6</b>	<b>58.4 ± 49.3</b>	0.0 ± 0.0	0.0 ± 0.0
ai3	0.0 ± 0.0	0.0 ± 0.0	0.0 ± 0.0	0.0 ± 0.0	<b>0.2 ± 0.5</b>	<b>13.0 ± 33.6</b>	0.0 ± 0.0	0.0 ± 0.0
f	0.0 ± 0.0	0.0 ± 0.0	0.0 ± 0.0	0.0 ± 0.0	0.0 ± 0.0	0.0 ± 0.0	0.0 ± 0.0	0.0 ± 0.0
inductive-inference	0.0 ± 0.0	0.0 ± 0.0	0.0 ± 0.0	0.0 ± 0.0	0.0 ± 0.0	0.0 ± 0.0	0.0 ± 0.0	0.0 ± 0.0
parity	0.0 ± 0.0	0.0 ± 0.0	0.0 ± 0.0	0.0 ± 0.0	0.0 ± 0.0	0.0 ± 0.0	0.0 ± 0.0	0.0 ± 0.0
Beijing								
Beijing	0.0 ± 0.0	0.0 ± 0.0	0.0 ± 0.0	0.0 ± 0.0	<b>14.8 ± 34.8</b>	<b>15.4 ± 36.1</b>	5.9 ± 15.7	<b>15.4 ± 36.1</b>

Table 4. Comparative table showing results on SATLIB benchmarks for four methods: Product Logic, Godel Logic, Gödel Trick Uniform, and Gödel Trick Logistic. Columns: S stands for Sample Solved (mean ± std of number of solved samples), B stands for Best Solution (mean ± std of number of problem solved by keeping the best results among the samples). Highest S and B in bold.